Title

Long-distance gene flow and contrasting population structures of reef-building corals and their algal symbionts inform adaptive potential across the Western Pacific

Authors

Hugo Denis[1,2,3*], Katharine E. Prata[4,5], Hisatake Ishida[6], Iva Popovic[4,5], Véronique J.L. Mocellin[4], Magali Boussion[1], Ilha Byrne[5], Steven W. Purcell[3], Line K. Bay[4], Gaël Lecellier[7], Cheong Xin Chan[6], Cynthia Riginos[4,5], Emily J. Howells[3,8†], Véronique Berteaux-Lecellier[1,†]

Affiliations

1 Santé des Ecosystèmes tropicaux (SantEco) EMR9001, CNRS, IRD, Univ. de Nouvelle-Calédonie, Univ. la Reunion, UMR 250 ENTROPIE, Noumea 98800, New Caledonia, France.

2 ED 129, SU Sorbonne Université, 4, Place Jussieu, 75252 Paris, France

3 National Marine Science Centre, Faculty of Science and Engineering, Southern Cross University, Coffs Harbour, NSW, Australia

4 Australian Institute of Marine Science, Townsville, QLD, Australia

5 School of the Environment, University of Queensland, Brisbane, QLD 4072, Australia

6 Australian Centre for Ecogenomics, School of Chemistry and Molecular Biosciences, The University of Queensland, Brisbane, QLD 4072, Australia

7 Institut de Sciences Exactes et Appliquées (ISEA) EA7484, 145, Avenue James Cook – BP R4 98 851 Nouméa, New Caledonia

8 Lizard Island Research Station, Australian Museum, Sydney, NSW 2010, Australia

[†]: These authors contributed equally to this work

Author list footnotes

1 Santé des Ecosystèmes tropicaux (SantEco) EMR9001, CNRS, IRD, Univ. de Nouvelle-Calédonie, Univ. la Reunion, NC–UMR 250 ENTROPIE, Noumea 98800, New Caledonia, France.

*Lead contact and Corresponding author: denis.hugo08@gmail.com

Key words

coral reefs, holobiont, population genomics, Symbiodiniaceae, gene flow, demographic history, Coral Sea, western Pacific

Abstract

The genetic diversity and connectivity of reef-building coral populations are key to their survival in warming oceans. Yet our understanding of corals' demographic resilience and adaptive potential is complicated by cryptic species diversity, wide geographic distributions, and complex coral-algal symbioses. To address these challenges, we investigated genetic connectivity and diversity of the broadcast-spawning coral *Acropora spathulata* and its associated Symbiodiniaceae across 29 reefs spanning the Great Barrier Reef, the Coral Sea, and New Caledonia, using whole-genome sequencing of 1,088 colonies. We identified four genetically distinct coral populations that diverged between 0.27 and 0.65 million years ago, likely due to geographic isolation across thousands of kilometers. These populations maintained asymmetrical gene flow along major ocean currents despite demographic isolation, and sustained large local effective population sizes (~2,900), supported by a high dispersal range of ~100 km per generation. In contrast, their Symbiodiniaceae partners varied over finer spatial scales, with five distinct *Cladocopium* taxa distributed along latitudinal and cross-shore gradients, likely driven by local environmental conditions. These results suggest that high dispersal capacity and large local population size promote demographic resilience within reef systems, while environment-specific symbioses and long-distance gene flow across reef-systems support adaptation and evolutionary rescue.

Introduction

Reef-building corals and their microbial symbionts constitute coral holobionts that are the foundation of biodiverse but threatened coral reef ecosystems (Souter et al., 2021). As tropical corals are declining globally, it is crucial to better understand the evolutionary, spatial and environmental processes that shape their population dynamics and resilience (Edmunds & Riegl, 2020; van Oppen & Gates, 2006). However, the widespread presence of cryptic coral diversity (Grupstra et al., 2024; Riginos et al., 2024), along with vast geographic ranges (Gleason & Hofmann, 2011), challenges our ability to determine the size and connectivity of coral populations. In addition, variability in symbioses between coral hosts and symbiotic microalgae from the family Symbiodiniaceae can affect holobionts' capacity to grow, survive and adapt under changing conditions (Bourne et al., 2016).

Population genomics, which investigates genome-wide molecular variation, can differentiate coral taxa that are indistinguishable based on morphological criteria (Bongaerts et al., 2021), or traditional population genetic markers such as microsatellites (Arrigoni et al., 2020; Meziere et al., 2024). Within coral species, it can provide a holistic view of spatial genetic variation patterns in both hosts and symbionts across their range (Fuentes-Pardo & Ruzzante, 2017). These analyses are essential to uncover the distinct scales at which gene flow, local adaptation and co-evolutionary dynamics influence holobionts adaptive responses.

Contemporary gene flow (over tens of generations) is crucial for coral demographic dynamics, particularly for the recovery of locally depleted coral populations following perturbations (Hock et al., 2017; Holbrook et al., 2018). To quantify its spatial extent, isolation-by-distance (IbD) theory provides a useful framework by estimating a generational gene dispersal distance (Rousset, 1997; Wright, 1946). Combining the slope of IbD with estimates of effective density, one can infer the generational mean axial dispersal distance (σ), over which most dispersal events occur, and vast differences in σ depending on reproductive modes and taxa have been described (Gorospe & Karl, 2013; Japaud et al., 2019; Meziere et al., 2025; Prata et al., 2024). To estimate effective density, the local effective

population size (N_e) is estimated and divided by the area the population occupies. Local N_e indicates the loss rate of genetic variation due to genetic drift at the scale where most breeding events occur (Waples, 2024). This standing variation on which natural selection acts, underpins adaptive potential (Fisher, 1930). Jointly estimating σ and N_e thus provides crucial information on the extinction risk of local coral populations (Hernández-Agreda et al., 2024) and the spatial scale of demographic replenishment (Gaines et al., 2010), both are essential for defining conservation units.

Over longer evolutionary time-scales, occasional long-distance dispersal can affect species range and adaptation to global changes (Clobert, 2012). However, methods based on high-level genetic differentiation cannot disentangle the effect of migration from genetic drift and shared ancestry, or determine direction of gene flow (Lawson et al., 2018; Whitlock & McCauley, 1999). Demographic history inference approaches that model divergence times, variation in migration rates and long-term effective population sizes (Gutenkunst et al., 2009) offer a complimentary strategy to assess gene flow across a coral species range (Meziere et al., 2025). However, despite potential for coral connectivity spanning thousands of kilometers (Davies et al., 2015; Matz et al., 2018), such methods have been mostly applied within national borders (Matz et al., 2018; Meziere et al., 2025; Tsuchiya et al., 2022; Zhang et al., 2022). This limits the development of coordinated regional conservation strategies that incorporate gene flow from different regions to assess evolutionary adaptation potential of corals (Colton et al., 2022).

Importantly, coral evolution and conservation require consideration of their symbiosis with Symbiodiniaceae microalgae (LaJeunesse et al., 2018) that are genetically and physiologically diverse (Nitschke et al., 2022). For instance, photosynthetic ability of Symbiodiniacae is known to differ among taxa under heat stress (Levin et al., 2016); some taxa inhabit warmer environments (McRae et al., 2023) or increase in prevalence during thermal stress (LaJeunesse et al., 2009). Most Symbiodiniaceae are facultative symbionts, therefore both macro-environments and host micro-environments will favor certain taxa or genotypes (Bhattacharya et al., 2024; Quigley et al., 2019; Reich et al., 2021). In turn, some symbiont taxa may facilitate corals' local adaptation to environmental conditions (Howells et al., 2012). Symbiont diversity has been mostly described using

101 phylogenetic markers such as the ribosomal internal transcribed spacer 2 (ITS2; Hume et al., 2019)
102 and the chloroplastic non-coding region of *psbA* gene, i.e., psbA^{ncr} (Moore et al., 2003), or via
103 multilocus genotyping (e.g., Davies et al., 2020; Lewis et al., 2024). Yet, distinguishing intra- from
104 inter-genomic variants remains challenging, and the dependence on few selected marker genes may
105 limit taxonomic resolution (Armstrong et al., 2024). Methods based on genome-wide sequence
106 composition of hologenome samples are thus emerging (Ishida et al., 2024), unlocking hidden
107 phylogenetic (Armstrong et al., 2024; Cooke et al., 2020; Zhang et al., 2022) and ecological (Hoadley
108 et al., 2021) diversity of these coral symbionts.

109 *Acropora spathulata* is a fast-growing, broadcast-spawning and widespread species that
110 inhabits shallow reef environments in the Western Pacific, including the Great Barrier Reef (GBR),
111 the Coral Sea, and New Caledonia (NC). Genomic data has revealed new insights into the cryptic
112 diversity of *Acropora* corals on the GBR (Matias et al., 2022; Naugle et al., 2024), their associated
113 Symbiodiniaceae (LaJeunesse et al., 2004; Matias et al., 2022; Naugle et al., 2024; van Oppen et al.,
114 2001) and realized connectivity, dominated by southward migration of coral larvae (Matz et al., 2018;
115 Riginos et al., 2019). However, such information remains scarce in NC with only one genomic study
116 conducted to date on *Acropora* coral hosts (Selmoni et al., 2021), and few on their symbiont
117 communities (Alessi et al., 2024; Camp et al., 2020; Denis et al., 2024b). In addition, despite being
118 one of the most studied coral reef ecosystem (Alvarado-Cerón et al., 2022), GBR's connectivity with
119 nearby western Pacific islands such as NC remains unknown. Several ocean currents flow westward
120 and eastward between the GBR and NC (Figure S1; Cravatte et al., 2015), offering potential for
121 periodical dispersal via stepping-stone migration through Coral Sea atolls, e.g. the Chesterfield-
122 Bellona (CB) plateau. To our knowledge, no study—in corals or other marine organisms—has
123 systematically assessed gene flow in this western Pacific region, aside from pumice rafting coral
124 larvae from NC to the GBR (Jokiel, 1990), and some genetic admixture between these reef systems
125 and Coral Sea atolls (Lukoschek et al., 2016; Oury et al., 2020). NC and the Southern GBR are often
126 considered potential climate refugia with projected stability of coral cover (Marzonie et al., 2025;
127 Matz et al., 2020; Sully et al., 2022) due to the mild occurrence of bleaching until recently (Shlesinger

128 & van Woesik, 2023). Understanding whether these systems have or still exchange migrants is
129 therefore important for their regional conservation.

130 Here, we systematically assess the host and symbiont population structures and gene flow of
131 the coral *Acropora spathulata*, expanding the common research scope of the GBR (Cooke et al., 2020;
132 Matias et al., 2022; Scott et al., 2024; van Oppen et al., 2018; Warner et al., 2015) to the Western
133 Pacific. By integrating existing and innovative genome-scale approaches, we densely sampled,
134 sequenced, and analyzed whole-genome sequencing data from 1,088 colonies from 29 reefs across the
135 GBR, the Coral Sea and NC. Our study represents one of the most geographically comprehensive
136 efforts to concurrently investigate coral host and symbiont diversity as well as contemporary and long-
137 term connectivity.

138

139 **Methods**

140 *Study sites and sample collection*

141 *A. spathulata* was sampled from the east coast of Australia to the west coast of New Caledonia and
142 across a 10 ° latitudinal gradient (Table S1). The first batch of samples consisted of 831 colonies
143 collected across 15 reefs of the Great Barrier Reef (*n* = 40–60 per reef; Figure 1) between 28 February
144 and 26 March 2022 (GBRMPA permit G21/45166.1) as described in Denis et al. (2024a). The second
145 batch comprised 323 colonies collected across 14 reefs of the western coast of New Caledonia (NC)
146 and atolls of the Chesterfield-Bellona (CB) plateau located in the Coral Sea (*n* = 4–25 per reef)
147 between 26 June and 28 September 2023 (New Caledonia Natural Park of the Coral Sea permit 2023-
148 1503/GNC, South Province permit 4508- 2022/ARR/DDDT and North Province permit 609011). At
149 each reef, small fragments (< 1 cm^3) were collected on SCUBA from coral colonies originating from
150 one or two sites (covering 50–4200 m^2) and immediately stored in 80–100% ethanol for DNA
151 extraction. Depending on reef sites geomorphology, colonies were collected from upper reef slopes,
152 fringing reefs, inner barrier reefs or reef flats at an average depth of 0.6 m (-0.7 m to 5.6 m relative to
153 the lowest astronomical tide). Geographic coordinates were recorded for each colony by carrying a

154 GPS in tow on a surface float (except at NC and CB reefs), and whole colony photographs and
155 macrophotographs were taken of each colony using an Olympus TG-6. The occurrence of clones was
156 minimized by avoiding sampling neighboring colonies of similar pigmentation.

157 *DNA extraction and sequencing*

158 Coral fragments from 1,154 colonies were used for DNA extraction and 1,144 high quality DNA
159 samples were used for library preparation and whole genome sequencing (Table S2). While extraction
160 and sequencing of the GBR and New Caledonia samples were conducted at different facilities, similar
161 extraction and library preparation kits and sequencing platforms were used in order to minimize batch
162 effects. In addition, a subset of 23 samples from the GBR were extracted and sequenced alongside both
163 batches to control for such effects (Supplementary Material and Methods). In both cases, total DNA was
164 extracted from coral tissue slurry (tissue and skeleton) using Qiagen DNeasy Blood and Tissue Kit
165 (Qiagen, Hilden, Germany) following manufacturer's instruction, including an RNAse digestion step
166 for GBR samples (30 min at room temperature). For GBR samples, sequencing libraries were prepared
167 using the Lotus DNA Library Prep Kit for NGS (10 ng of input DNA, 8 PCR cycles) and sequenced on
168 the Illumina NovaSeq 6000 platform (200 cycles; 150 bp paired end reads; targeting 10X coverage;
169 Azenta Life Sciences, CSIRO). For New Caledonia samples, the libraries were prepared using the
170 Truseq Nano DNA kit (200 ng of input DNA, 8 PCR cycles) and sequenced on the Illumina NovaSeq
171 X platform (300 cycles; 150 bp paired end reads; targeting 10X coverage; Macrogen, Korea).

172 *Genomic data pre-variant processing and filtering*

173 The bioinformatic pipeline used to process, filter, and analyze the genomic data is outlined in Figure
174 S2. The dataset consisted of the 1,144 sequenced individuals with technical replicates (n = 25;
175 Supplementary Material and Methods). Pre-variant filtering steps are summarized in Table S2.
176 Adapter removal and read quality trimming was conducted using *Trimmomatic* v0.39 (Bolger et al.,
177 2014) with a 4 bp sliding window, a minimum phred score quality of 20, and a minimum read length
178 of 50 bp. Leading and trailing low quality bases were removed (LEADING:3, TRAILING:3) and
179 adapter sequences were removed using the Illuminaclip option in 'palindrome mode' (2:30:10:4).
180 Sample quality was confirmed using *FastQC* v0.12.1

181 (http://www.bioinformatics.bbsrc.ac.uk/projects/fastqc) and *MultiQC* v1.21 (Ewels et al., 2016).
182 Filtered reads were then aligned to the *Acropora millepora* reference genome v3 assembly
183 (unpublished upgrade from GCA_013753865.1_Amil_v2.1; see Supplementary Material and Methods
184 for a justification of the reference genome choice) using the *Burrow-Wheeler Aligner* v0.7.17 (Li &
185 Durbin, 2010) and the *MEM* algorithm at default settings. SAM files were converted to indexed and
186 sorted BAM files using *Samtools* v1.20 (Danecek et al., 2021) and PCR duplicates were marked and
187 removed using *Picard* v3.1.1 (VALIDATION_STRINGENCY=LENIENT;
188 http://broadinstitute.github.io/picard/). After filtering of samples that failed to be sequenced and
189 samples with unexpectedly low percentage (< 80%; possibly indicative of mis-identified taxa) or
190 number (< 10M) of mapped reads, 1,132 BAM files were retained. To provide an initial evaluation of
191 population structure across the study system and pinpoint potential clones and taxa misidentification,
192 this dataset was analyzed with a genotype likelihood framework in *ANGSD* v0.940 (Korneliussen et
193 al., 2014; see Supplementary Material and Methods for results). Four samples from the GBR and 23
194 samples from NC were discarded as they likely belonged to *A. millepora* and a distinct unknown
195 taxon, respectively.

196 *SNPs calling, clone identification and filtering*

197 Indexed, duplicate-free BAM files were used to call variants and genotypes from a total of 1,105
198 remaining samples using *GATK* v4.5.0.0 'Germline short variant discovery best practice' workflow
199 (Van der Auwera & O'Connor, 2020). Variant calling was first performed per sample, focusing only
200 on reads mapping to the 14 reference chromosomes, using the *HaplotypeCaller* tool that performs *de*
201 *novo* assembly of haplotypes in active regions. Individual 'gvcf' files were then consolidated per
202 chromosome using *GenomicDBimport* and used for joint genotyping using *GenotypeGVCFs* tool.
203 *GatherVCFs* and *SelectVariants* tools were used to combine chromosome files in a single variant call
204 format (VCF) file and separate SNPs from INDELs and monomorphic sites. The SNPs VCF file was
205 preliminarily filtered using *GATK VariantFiltration* tool following GATK stringent filtering best
206 practices (QD > 2, FS < 50, MQ > 40, MQRankSum > -12.5, ReadPosRankSum > -8, SOR < 3, GQ >
207 20) and 17 individuals with high missingness (> 85%) were discarded. Previously identified putative

208 clonal colonies were confirmed and filtered to retain only one colony with the lowest missingness per
209 clonal group (Supplementary Material and Methods, Table S3).

210 *Host population genomics analyses*

211 To confirm the absence of strong batch effects that could confound population structure, a subset of 23
212 technical replicates pairs was sequenced along both GBR and NC samples (Supplementary Material
213 and Methods; Figure S3). After exclusion of natural clones and technical replicates, a final set of 999
214 individuals was used for host population genetic analyses. A first dataset of unlinked SNPs was
215 created to investigate population structure and phylogenetic relationship between populations of the
216 Coral Sea, retaining only bi-allelic SNPs with a minimum mean locus depth of 5 and a maximum of
217 15, a minor allele frequency (MAF) > 0.05 and a locus missingness < 20% with *vcftools* v0.1.17
218 (Danecek et al., 2011). In addition, SNPs in linkage disequilibrium with a pairwise $r^2 > 0.2$ were
219 removed using *plink* v1.90b7.2 (Purcell et al., 2007; "Dataset 1", Table S4) because we were
220 interested in identifying neutral population structure patterns that occur throughout the genome. To
221 identify genetically distinct groups of individuals, we performed a principal component analysis
222 (PCA) with the *glPca* function from R package *adegenet* v2.1.10 (Jombart, 2008). We then estimated
223 individual ancestry proportion using ADMIXTURE v1.3.0 (Alexander & Lange, 2011). The optimal
224 number of ancestral populations (K=4) was determined using the cross-validation method
225 implemented in ADMIXTURE. Following Hemstrom et al. (2024) best practices, these analyses were
226 also conducted using variable stringency MAF (MAF > 0.01 and MAF > 0.05) and missingness
227 thresholds (5%, 10%, 20% and 50%).

228 Finally, we used a subset of individuals with the highest ancestral assignment in ADMIXTURE (200
229 colonies, 50 colonies per population) and built an individual-based Maximum Likelihood phylogenetic
230 tree using RAxML (Stamatakis, 2014). To build the tree, the VCF file was converted to the Phylip
231 format using *vcf2phylip.py* script (https://github.com/edgardomortiz/vcf2phylip) and raxmlHPC-
232 PTHREADS was run with a GTRGAMMA model and 100 bootstrap replicates.

233 *Population statistics*

234 A second dataset of linked SNPs was used to compute population genetic differentiation and diversity
235 estimates retaining SNPs with a minimum mean locus depth of 5 and a maximum of 50, a minimum
236 allele count (MAC) of 1, a *p*-value of deviation from HWE test >0.0001 and < 20% missingness
237 ("Dataset 2", Table S4) following recommendations of Hemstrom et al. (2024). To generate unbiased
238 estimates of population genomic statistics despite missing data, the SNP dataset was concatenated to
239 include invariant sites, filtered with the same depth and missingness thresholds per above, and used to
240 compute statistics with *pixy* v1.2.10 (Korunes & Samuk, 2021). Following Sopniewski and Catullo
241 (2024), 10 replicates of 5 randomly selected individuals per population were used to compute the
242 fixation index (F_{st}) using the Weir and Cockerham method (Weir & Cockerham, 1984). Because F_{st}
243 estimates can be affected by within population diversity, we also computed absolute divergence (D_{xy})
244 for each replicate, to get more-independent estimates of population differentiation. Finally, we
245 computed nucleotide diversity (π) within each population. We reported the median F_{st}, D_{xy} and π
246 estimates across replicates.

247 *Demographic modeling*

248 To investigate the evolutionary history and connectivity of these populations, a subset of Dataset 2
249 comprising 120 colonies (30 colonies per population, showing >95% admixture cluster assignment)
250 was used to conduct demographic modeling analyses in *dadi* v2.3.3 (Gutenkunst et al., 2009). This
251 dataset was further filtered to retain SNPs with a minimum allele count (MAC) of 3 to minimize the
252 effect of sequencing errors. SNPs showing a deviation from HWE (*p*-value < 0.0001) were also
253 removed as we observed an excess in heterozygosity creating a peak in the SFS at 0.5 haplotype
254 frequency, potentially due to gene duplication, paralogous loci or balancing selection. Finally, a
255 second round of filtration to ensure < 20% missingness within each population was performed using
256 *vcf_minrep_filter.py* script (https://github.com/pimbongaerts/radseq, "Dataset 3", Table S4). VCF files
257 were created for each population pair (n=6) and analyzed using a custom workflow to estimate
258 effective population sizes, divergence time and migration rates between populations
259 (https://github.com/kepra3/kp_dadi).

260 We computed joint-allelic frequency spectrums (JAFS) for each pair using the subsample method to
261 account for missing data, and masking singletons and doubletons to minimize the effect of sequencing
262 errors or somatic mutations. We initially tested three scenarios; divergence in isolation, divergence
263 with asymmetrical migration and ancestral asymmetrical migration. We optimized the models'
264 parameters to best fit the observed JAFS (Figure S4). To avoid getting stuck in local optima,
265 optimization was performed by exploring the parameter space in three stages: first with three-fold,
266 then two-fold, and finally one-fold perturbations of the starting parameters, based on the previously
267 optimized peak values (>100 runs per stage). The final set of parameters was chosen when appearing
268 several times with 1-fold perturbation from different initial values. To get confidence intervals for
269 these parameters, 100 bootstraps were created for each pair by resampling genomic contigs.
270 Optimization runs (n=50) were performed for each bootstrap and model, using 1-fold perturbations
271 starting from previously optimized parameters. For each bootstrap replicate, delta-AIC values were
272 computed between models, and the mean delta-AIC across replicates was used to identify the best-
273 fitting model for each population pair (Figure S5). Optimized parameters from the best-fitting model
274 (divergence with asymmetrical migration) were used to calculate 95% credible intervals, after
275 excluding bootstrap replicates within the lowest 10% likelihood quantile.

276 Finally, we converted parameter values obtained in *dadi* (θ, ν_{1dadi}, ν_{2dadi}, M_{12dadi}, M_{12dadi} and
277 T_{dadi}) into physical units: divergence time in years, effective population sizes in number of
278 individuals and gene flow between taxa in number of migrants per generation. To do so we first
279 calculated the effective sequence length for each pair as:

280 $$L = \frac{SNP_{dadi}}{SNP_{detected}} \times N_{sites}$$

281 where SNP_{dadi} is the number of SNPs used to construct the JAFS from the specific pair, $SNP_{detected}$
282 is the number of SNPs originally detected before filtration, and N_{sites} is the number of sites obtained
283 from GATK pipeline (including SNPs, INDELs and monomorphic sites). Next, we computed the
284 ancestral population size (N_{ref}) and the effective population sizes ν_1 and ν_2 in number of individuals,
285 the divergence time (T) in years, migration rates in fraction of migrant individuals at each generation

(m_{12} ; from Population 2 to Population 1 and m_{21}; from Population 1 to Population 2) and rates of gene flow in number of individuals per generation (M_{12} and M_{21}), using the following formulas:

$$N_{ref} = \frac{\theta}{4 \times \mu \times L}$$

$$T = 2 \times T_{gen} \times N_{ref} \times T_{dadi}$$

$$\nu_1 = \nu_{1dadi} \times N_{ref}$$

$$\nu_2 = \nu_{2dadi} \times N_{ref}$$

$$m_{12} = \frac{M_{12dadi}}{2 \times N_{ref}}$$

$$m_{21} = \frac{M_{21dadi}}{2 \times N_{ref}}$$

$$M_{12} = m_{12} \times \nu_1$$

$$M_{21} = m_{21} \times \nu_2$$

We used a mutation rate μ of 1.2×10^{-8} mutations per base per generation, previously estimated for *Acropora* corals (Zhang et al., 2022) and a generation time T_{gen} of 5 years following the assumptions of Matz et al. (2018) on generation times of *A. millepora*.

Isolation by distance analysis and estimating N_e

To estimate realized dispersal and effective population sizes, Dataset 2 was further filtered to retain SNPs with <10% missing data and physically pruned to remove SNPs separated by <500 bp ("Dataset 4"). This was done because both isolation by distance (IbD) analyses and N_e estimation methods require no physical linkage (Waples, 2024).

Using this dataset, we estimated σ that represents ecologically relevant gene flow averaged across the last 10–15 generations, following Prata et al. (2024) with modifications. Multiple IbD regressions were performed in *spagedi* v1.5 (Hardy & Vekemans, 2002) using the empirical estimate of Rousset's individual genetic distance (â; Rousset, 1999) and the geographic distance between individuals.

308 Geographic distances were calculated using the Haversine formula, that estimates great-circle
309 distances between latitude-longitude pairs. Regression analysis conducted within each of the four
310 populations (corresponding to geographic regions; Figure 1) revealed no significant IbD. Because we
311 were interested in a general dispersal estimate across the species range and the F_{st} estimates amongst
312 populations were low, we used the global dataset for conducting the IbD analysis. Different
313 regressions were performed to estimate the slope β for a range of spatial scales that roughly evenly
314 partitioned the dataset (maximum distance 50 m to 2,300 km). We queried multiple spatial scales in
315 order to select *a posteriori* the appropriate regression distance spanning minimum σ and maximum
316 10–50 σ following Hardy and Vekemans (1999). The dimensionality of the habitat was determined for
317 each regression by the width to area ratio, using a 1D analysis for a ratio <0.1 and a 2D analysis and
318 the $\log_{10}$ of geographic distance for a ratio >0.1 (Rousset, 1997). Similarly, for multiple spatial scales,
319 the population density (D_e) was estimated by dividing the effective population size by the habitat area
320 (A) for 2D or length (L) for 1D regressions (see below). Confidence intervals for β were estimated
321 using a jackknifing procedure across individuals and the slope was deemed significant when the
322 confidence intervals did not span 0. All β and D_e estimates were then combined to estimate σ at each
323 spatial scale using the following isolation-by-distance model equation (Rousset, 1997; Wright, 1946),
324 example for two-dimensions:

325 $$\sigma = \sqrt[2]{\frac{1}{\beta 4\pi D_e}}$$

326 The linkage disequilibrium method was used to estimate the effective population size (N_e) at the
327 neighborhood extent (radius of 2σ), which N_e represents the effective number of individuals that can
328 easily mate in a continuously distributed population (N_b; Neel et al., 2013). Neighborhood N_e was
329 estimated using *LDNe* v2.1 (Waples & Do, 2008) with a minimum allele frequency filter based on the
330 number of samples following authors recommendations. Confidence intervals were obtained for N_e
331 using the jackknifing procedure.

332 Finally, we filtered our β, σ and N_e estimates to ensure that the spatial scales at which the IbD
333 regression was performed matched a σ value ranging from σ to 10–50σ following Hardy and

334 Vekemans (1999). We also removed any instance where N_e was not estimated at the neighborhood
335 area, A or L equating to $4\pi\sigma^2$ for two dimensional habitat (or $2\sqrt{\pi}\sigma^2$ for one dimension) because this
336 is the ideal spatial scale to estimate N_e (Neel et al., 2013). Upper and lower confidence intervals for
337 filtered estimates were then used to obtain distributions of β and N_e through resampling (n=100). A
338 gamma distribution was used for N_e and a log-normal distribution for β. These distributions were then
339 combined to create a joint σ distribution and propagate the error from each separate analysis.

340 *Symbiodiniaceae community analyses*

341 We used genomic reads from 1,088 *A. spathulata* holobionts to characterize symbiont community
342 composition and diversity across our study area, adopting the approach by Ishida et al. (2024),
343 available at https://github.com/hisatakeishida/Symb-SHIN. Genomic reads not mapping to the host
344 reference genome (i.e. non-coral reads) were first re-aligned to several reference genomes of
345 Symbiodiniaceae using the Burrow-Wheeler Aligner v0.7.17(Li & Durbin, 2010) and the MEM
346 algorithm (*bwa-mem*) at default setting, with one reference per genus (*Symbiodinium microadriaticum*
347 CCMP2467 (Nand et al., 2021), *Breviolum minutum* Mf1.05b (Shoguchi et al., 2013), *Cladocopium*
348 *proliferum* SCF055-01 (Chen et al., 2022), *Durusdinium trenchii* CCMP2556 (Dougan et al., 2024),
349 *Effrenium voratum* RCC1521 (Shah et al., 2024) and *Fugacium kawagutii* CCMP2468 (Li et al.,
350 2020)).

351 For the first-pass analysis of the symbiont community composition, we retrieved and classified ITS2
352 sequences present in the samples using *graftM* (Boyd et al., 2018). All ITS2 sequence variants were
353 classified as belonging to genus *Cladocopium*. Consequently, to improve intra-specific taxonomic
354 resolution we also analysed $psbA^{ncr}$ sequences among the samples. We retrieved $psbA^{ncr}$ sequences by
355 mapping reads to a custom $psbA^{ncr}$ reference database using *bwa-mem*. We then follow Armstrong et
356 al. (2023) to retain only reads that aligned in full length (100% cover) at >90% identity, and used
357 number of uniquely mapped reads as proxy for abundance.

358 To capture genetic diversity of symbionts directly using whole-genome sequencing data not restricted
359 to selected marker genes, we adopted a *k*-mer-based alignment-free approach, following earlier studies

360 (Ishida et al., 2024; Zhang et al., 2022). The *k*-mers in each sample were first enumerated using
361 *jellyfish* v1.1.12 (https://github.com/gmarcais/Jellyfish) at $k = 21$ yielding a 21-mer profile following
362 previous studies (González-Pech et al., 2021). Pairwise distance between samples was computed from
363 these profiles using *d2ssect* (https://github.com/bakeronit/d2ssect), based on D_2^s metric (Reinert et al.,
364 2009). Samples containing similar symbiont compositions are expected to share similar *k*-mer profiles
365 (i.e., short D_2^s-derived distance).

366 To validate the aforementioned methods using a conventional amplicon-based approach, a subset of 36
367 DNA samples distributed across host populations (Figure S6) were used for ITS2 marker amplification
368 (Herculase II Fusion DNA Polymerase Nextera XT Index V2 Kit) and Illumina sequencing at
369 Macrogen (Seoul, Korea) using forward primer SYM_VAR_5.8S 5'-
370 GAATTGCAGAACTCCGTGAACC-3' and reverse primer SYM_VAR_REV 5'-CGGGTT
371 CWCTTGTYTGACTTCATGC-3′ (Hume et al., 2018). ITS2 sequence data was submitted to the
372 SymPortal analytical framework (https://symportal.org; Hume et al., 2019) and ITS2 sequence variants
373 and type profiles output by the pipeline were used to visualize the results. For this subset of 36
374 individuals, *graftM* results were checked for consistency with SymPortal results using a relative
375 abundance barplot of ITS2 sequence variants. Using the same set of samples, we also compared the
376 hierarchical clustering of Unifrac distances based on ITS2 'defining intragenomic variants' with that
377 based on D_2^s distances, which showed great consistency (Figure S7) and thus we assigned each of the
378 D_2^s clusters the corresponding major ITS2 sequence. Both dendrograms were aligned to build a
379 tanglegram with R package *dendextend* and the stepside method (Galili et al., 2015).

380 *Host and symbiont co-clustering analysis*

381 To visualize how Symbiodiniaceae communities varied across host populations, we performed a
382 hierarchical clustering of samples using the pairwise distance matrix derived from the D_2^s metric
383 (above) using all samples ($n = 878$) for which > 50 M bp of reads mapped to the reference
384 Symbiodiniaceae genomes. This dendrogram was pruned to build a tanglegram with the host
385 phylogenetic tree obtained in *RAxML* using *dendextend*.

386 *Distance based redundancy analysis*

387 We first investigated the influence of geography and environmental conditions on the global host
388 population structure of *A. spathulata* across the Western Pacific (N=999). For this purpose, we
389 retrieved environmental predictors from several satellite products and models with a focus on variables
390 known to be primary drivers of coral holobiont community composition (temperature, light and
391 turbidity; Supplementary Material and Methods, Table S5). We modeled spatial relationships among
392 colonies using distance-based Moran's Eigenvector Maps (dbMEMs), which capture multi-scale
393 spatial relationships using principal coordinate analyses (Borcard & Legendre, 2002). As individual
394 colony-level GPS coordinates were not recorded at NC and CB reefs, randomly jittered coordinates
395 within 300 m around the reef coordinate (recorded using a GPS during sampling; corresponding to the
396 approximate size of the sampling area) were assigned to each colony at these reefs. The neighbor
397 matrix for each colony was computed from spatial coordinates using Haversine distance in R package
398 *geosphere* (Hijmans et al., 2017) and used to compute dbMEMs eigenvectors using R package
399 *adespatial* (Dray et al., 2018). The first four eigenvectors associated with positive eigenvalues were
400 kept in further analyses based on a screeplot of cumulative variance explained (>95%). All predictors
401 were standardized by subtracting the mean and dividing by the standard deviation to ensure
402 comparable units.

403 We performed a redundancy analysis (RDA; Legendre & Anderson, 1999) using R package *vegan*
404 (Oksanen et al., 2013). The first RDA model was built using the first 10 principal components of the
405 PCA on host SNPs as a dependent matrix, and all environmental variables as predictors. Collinear
406 predictors were removed successively, starting with the variables with the highest variance inflation
407 factor (VIF), recomputing the model VIF and repeating this procedure until all predictors had a VIF <
408 10. Model significance was tested using an analysis of variance (ANOVA) and individual axes
409 significance was tested using an ANOVA-like permutation test in package *vegan* with 500
410 permutations per axis. Forward selection was used to select predictors that were statistically
411 significant. We used the framework developed by Capblancq and Forester (2021) to assess the relative
412 influence of geography and environment on host structure. We built a global RDA model using (1)

413 environmental variables previously identified as significant using forward selection and (2) the first
414 four dbMEM eigenvectors as predictors. Separate partial RDA models were built setting either
415 environmental variables or spatial eigenvectors as conditional variables (i.e., 'partialled out'). Model
416 significance was tested using an ANOVA and models were compared based on inertia, total variance
417 explained, and proportion of constrained variance explained.

418 We used a similar approach to investigate the influence of geography, environmental factors and host
419 population structure on the differentiation of *A. spathulata* symbiont communities (*n*=878) which are
420 horizontally acquired (van Oppen et al., 2001). Our preliminary analysis showed that ordinations
421 based on *k*-mer-derived D_2^s distance were influenced by the number of symbionts reads in each
422 sample, therefore all samples were downsampled to 50 M bp and samples below this threshold were
423 discarded (10% of samples). As a small effect on the ordination remained, we included this variable as
424 a conditional variable in all of our models. We performed a principal coordinate analyses (Borcard &
425 Legendre, 2002) on the *k*-mer-derived D_2^s distance matrix and used the first 10 principal coordinates
426 as a dependent variable in RDA models. As the PCoA did not yield negative eigenvalues indicating
427 the distance matrix was nearly Euclidean, we did not perform negative eigenvalues correction as
428 routinely applied in dbRDA. The first RDA model was built using all environmental variables and
429 significant predictors were selected following the same procedure as above. A second global RDA
430 model was built using (1) environmental variables previously identified as significant using forward
431 selection, (2) the first four dbMEM eigenvectors and (3) the first three host PCs as predictors
432 (explaining almost all of the variation; Figure S8). The marginal effect of each category of predictor
433 was then assessed through separate pRDA models, using the two other categories as conditional
434 variables. All statistical analysis were conducted using *R* v4.0.4 and figures created using package
435 *ggplot2* (Wickham, 2011).

436 **Results**

437 *Genomic data processing and filtering*

438 We recovered 339,720 single nucleotide polymorphisms (SNPs) from 1,088 individual coral colonies
439 of *Acropora spathulata* using a stringent filtering approach (see Methods). This dataset had a mean
440 locus-level sequencing depth of 13.7 ± 1.2 (mean ± sd). Following removal of related individuals and
441 linked SNPs, Dataset 1 used for population structure analyses comprised 999 individuals and 27,175
442 SNPs. Dataset 2 used to compute genetic differentiation and diversity metrics consisted of ~2.2 M loci
443 (SNPs and monomorphic sites). Dataset 3 used for demographic modeling consisted of 37,841–61,902
444 SNPs per population pair and Dataset 4 used for IbD analyses and N_e estimates consisted of 2,011
445 SNPs after pruning for physical linkage.

446 *Coral host population structure*

447 *A. spathulata* colonies across the Western Pacific were separated into four genetically differentiated
448 groups, hereinafter referred to as populations (Figure 1). A PCA revealed geographically distinct
449 populations separated on PC1 and PC2 (1.5% and 0.7% explained variance respectively; Figure 1a),
450 corresponding to the Central to Northern GBR (i.e., from Davies to Hicks reefs), the Southern GBR,
451 the Chesterfields-Bellona atolls (CB) in the Coral Sea and the western New Caledonia's main island
452 (NC). PC3 (0.5% explained variance, Figure 1a) separated the CB group from the three other groups.
453 Similarly, ADMIXTURE analysis found a concordant optimal number of $K = 4$ ancestral populations
454 (Figure S9, Figure S10). The separation of individuals by their ancestry proportion was consistent with
455 PCA results but revealed small levels of admixture between all populations (Figure 1b). In particular,
456 4 of 137 and 19 of 137 colonies found in the Southern GBR had a >0.5 and >0.25 assignment to the
457 ancestral population of the Central/Northern GBR respectively.

458 *Population divergence and genetic diversity*

459 Genetic divergence, estimated using the fixation index, was low between all of the four populations
460 ($F_{st} < 0.030$; Table 1) and was the lowest between the two GBR populations ($F_{st} = 0.014$). Pairwise D_{xy}
461 ranged from 0.010 to 0.011 and was the lowest between the NC and CB populations. This corresponds
462 to an average 1% nucleotide difference per bp between populations (Table 1). Nucleotide diversity (π)
463 was the highest in the NC population ($\pi = 0.0106$) followed by the Central/Northern GBR ($\pi = 0.0103$)

464 and the Southern GBR populations (π = 0.0100). The CB population appears to have the lowest
465 nucleotide diversity (π = 0.0097).

466 *Dispersal and effective population size*

467 No significant IbD occurred within populations. However, the pattern of IbD was revealed when
468 populations were analyzed jointly, with the regression of individual Rousset's genetic distance on
469 geographic distance yielding a significant positive slope ($\beta = 0.00064 \pm 3.7 \times 10^{-05}$; median ± sd;
470 Figure 2a). The effective population size at the neighborhood size across this geographic range was
471 estimated at N_e = 2,954 ± 1,573 effective individuals (median ± sd; Figure 2b). Combining these
472 estimates, the average dispersal distance between parents and offspring across generations was 109 ±
473 33 km (mean axial dispersal distance; σ; median ± sd; Figure 2c).

474 *Demographic modeling of populations divergence and gene flow*

475 For all population pairs, observed joint allelic frequency spectrum (JAFS) were best explained by
476 demographic models consisting of divergence with asymmetrical gene flow than models with no gene
477 flow or ancestral gene flow (Figure S5). This suggests that these populations have diverged across the
478 western Pacific while exchanging larvae over many generations. Demographic models estimated
479 divergence time between 275 to 651 thousand years ago depending on population pairs (Table 1),
480 although these are approximate estimates because germline mutation rates are lacking for this species.
481 Based on these estimates, the two populations from the GBR appear to have diverged most recently
482 (275 [230–319] kya; median [5–95%]). Modelling results suggest that divergence of NC from other
483 populations (323–651 kya) is more ancient than divergence of CB from GBR populations (354–385
484 kya). However, large overlap in confidence intervals, and possible bias introduced by high migration
485 rates, make it difficult to reconstruct their precise sequential divergence history.

486 Migration rates and gene flow rates were asymmetrical for most population pairs, and this result was
487 consistent across bootstrap replicates and optimization runs (Table 1). On the GBR, migration rates
488 were on average 5 times higher from the Central/Northern population to the Southern population (2.5
489 $\times 10^{-04}$) than vice versa (6.2×10^{-05}), resulting in higher southward gene flow (N_em) in line with

490 predominant oceanographic currents (Figure 1c; Figure S1). Eastward migration rates from both GBR
491 populations to the CB population (9.3×10^{-05}–1.2×10^{-04}) were higher than the westward rates ($5.4 \times$
492 10^{-05}–1.2×10^{-04}). However, differences in long-term effective population sizes (29,000–66,000
493 effective individuals) resulted in nearly symmetrical gene flow between the GBR and these Coral Sea
494 atolls (6.5–7.1 migrants per generation, Figure 1c). Migration rates between the CB and NC
495 populations were broadly symmetrical (6.5–7.0×10^{-05}), but the compounding effect of unequal
496 population sizes produced a dominance of eastward gene flow (11.0 [9.8–12.1] migrants per
497 generation; median [5–95%]). Gene flow was also directed primarily eastward, from both GBR
498 populations toward NC (Figure 1c).

499 *Symbiodiniaceae genetic diversity based on molecular markers*

500 We mapped non-coral reads from our 1,088 hologenomes to Symbiodiniaceae reference genomes and
501 recovered a median of 708,000 Symbiodiniaceae reads per sample (range: 63,540 to 24,932,887). All
502 colonies harbored symbionts from the *Cladocopium* genus with predominant ITS2 sequence variants
503 (recovered from hologenome reads) classified as C50, C3 and *Cladocopium* sp. (Figure S11).
504 Hologenome sequencing results were consistent with amplicon sequencing results in a subset of 36
505 samples, although the latter showed a greater taxonomic resolution, separating profiles dominated by
506 C3k, C3k/C3bo, C50b, and C50c sequences (Figure S6). Read mapping against *psbA*^{ncr} sequences
507 revealed classifications of *C. vulgare* (C1) or *C. sodalum* (C3; Figure S11). The mapping of reads to
508 *psbA*^{ncr} C1 in samples associated with C50 ITS2 sequences was presumably due to the lack of
509 reference *psbA*^{ncr} sequences of *Cladocopium* C50, limiting the use of this method for finer taxonomic
510 classification. However, our results suggest that the C3 symbionts identified are more closely related
511 to *C. sodalum* than other described C3 species (>80% of mapped sequences; Butler et al., 2023).

512 *Symbiodiniaceae community divergence based on k-mer profiles*

513 Alignment-free clustering of symbiont reads revealed some extent of co-clustering between each of the
514 four main symbiont taxa and the corresponding host populations (Figure 3). The host population in the
515 Central/Northern GBR was associated predominantly with *Cladocopium* taxa from C3k and C50c

516 subclades, with a cross-shore partitioning of these communities. Offshore reefs were associated with
517 C3k, while inshore reefs were associated with C50c (Figure 4a). At intermediate reefs (e.g., Moore,
518 North Direction, Mackay), some colonies harbored the C50c taxon while others harbored C3k. The
519 host population in the Southern GBR associated with a symbiont taxon of the C50b subclade. A few
520 colonies associated with C3k at Lady Musgrave Island. Corals in Western NC were predominantly
521 associated with a taxon from the C3k/C3bo subclade. The exception was some colonies in most
522 southern reefs which associated with a distinct symbiont taxon from C50b subclade. Based on ITS2
523 profiles, *k*-mer profiles clustering and geographic separation, this symbiont taxon is likely genetically
524 differentiated from the C50b taxa found in the Southern GBR (Figure S6 and S7). Coral hosts in the
525 CB atolls were also associated with a C3k/C3bo taxon that was indistinguishable from NC C3k/C3bo
526 despite being separated by >400 kilometers.

527 *Drivers of host and symbiont genetic structure*

528 The RDA indicated that environmental variables significantly predicted coral host genetic structure
529 (ANOVA; p-value < 0.01), explaining 64% of the total variance. Maximum monthly mean (MMM)
530 sea temperature, the frequency of mild marine heatwaves (DHW > 4), and distance to coast were the
531 strongest reef-level environmental predictors of host population structure (cumulative adjusted R^2 =
532 0.60, Table 2). A global RDA including geographic predictors (dbMEMs) on top of significant
533 environmental variables explained 70% of the total variance in host genetic structure. Due to the
534 spatial sampling design, several partial-RDAs indicated that environmental and geographic effects
535 were largely confounded (86% of explained variance).

536 Environmental predictors also significantly influenced the community composition of *Cladocopium*
537 symbionts (ANOVA; p-value < 0.01), explaining 37% of the total variance. The maximum monthly
538 Mean (MMM), frequency of mild marine heatwaves (DHW > 4) and annual range in sea surface
539 temperature (AR) were retained as significant predictors in the model (p-value = 0.001). The AR
540 separated C3 populations, found in more thermally variable environments at inshore and high latitude
541 reefs, from C50 populations found in offshore and low-latitude reefs (Figure 4b). Within the C50
542 subclade, distinct C50b and C50c populations were separated primarily by the MMM reflecting both

543 temperature variation across latitudinal gradient and cross-shore gradients. Within the C3 subclade, the
544 C3k populations were positively associated with the MMM, while C3k/C3bo populations were found
545 in reefs where MMM was lower on average, but where mild marine heatwaves have been more
546 frequent. Several pRDAs indicated that the environment was the strongest driver of symbiont
547 community composition (6.3% of total explained variance). Geography (1.2%) and host population
548 structure (1%) were less influential, although the effect of these three components was also largely
549 confounded (80% of explained variance, Table 2).

550 **Discussion**

551 Out results revealed four genetically distinct *A. spathulata* populations in the studied western Pacific
552 region, which have diverged due to geographic isolation but maintain gene flow through major
553 oceanographic currents. These populations show little genetic structure over distances greater than 500
554 km, reflecting a generational dispersal distance estimated at ~100 km. In contrast, coral hosts are
555 associated with distinct algal symbionts of five Symbiodiniaceae taxa across shorter latitudinal and
556 cross-shelf gradients. This study presents one of the most extensive datasets for analyzing spatial
557 genetic variation in both corals and their algal symbionts using whole-genome sequences, combining
558 broad geographic coverage and dense local sampling. These results suggest that large local
559 populations and dispersal support resilience of a broadcast-spawning coral, whereas habitat-specific
560 symbionts and long-distance gene flow could enhance its adaptive potential in changing environments.

561 *Regional spatial genetic variation differs among holobiont partners*

562 The spatial scale of genetic variation differed markedly between *A. spathulata* and its associated
563 *Symbiodiniaceae*. This coral species comprised four genetically differentiated populations distributed
564 in distinct regions separated by ~600–2,200 km. However, each population was largely genetically
565 homogenous based on PCA, ADMIXTURE and isolation-by-distance analyses, despite spanning up to
566 >300km for NC and CB, and up to >500km for the Central/Northern GBR. Conversely,
567 Symbiodiniaceae community genetic variation occurred over spatial scales as small as 30km, and

colonies from the same reef sometimes hosted distinct symbiont taxa. These patterns reflect the predominant effect of distinct evolutionary forces acting on holobiont partners.

Patterns of *A. spathulata* genetic variation suggest extensive gene flow promotes genetic homogenization of populations, counteracting the effects of drift and local adaptation (Slatkin, 1987). This was supported by our estimated σ exceeding >100 km. Across the distant western Pacific populations, reduced gene flow and increasing environmental contrasts (e.g., Δ~3°C in MMM; Figure S1) drive greater genetic differentiation (D_{xy} = 0.0102–0.0107). However, the relative importance of genetic drift and local adaptation in this differentiation could not be disentangled due to spatial confounding between environmental and geographic predictors (Table 2).

Patterns of Symbiodiniaceae genetic variation suggest that environmental filtering is the predominant driver of *A. spathulata* algal symbioses. Variation in symbiont communities was likely not strongly influenced by dispersal, as it did not follow an IbD pattern. For instance, colonies from Martin and No Name reefs (30km apart) hosted different taxa, while those from No Name and Chicken reefs hosted the same taxa (500km apart; Figure 4). In addition, the environment had a larger effect on symbioses than host genetic differentiation (although largely confounded; pRDA; Table 2), as expected from species that acquire symbionts from their environment after settlement (Davies et al., 2020; van Oppen et al., 2001). Variation in symbioses was particularly pronounced across shelf and latitudinal gradients, similar to other *Acropora* species on the GBR (Cooke et al., 2020; LaJeunesse et al., 2004; Matias et al., 2022). Notably, *A. spathulata* and *A. tersa* (formerly *A. hyacinthus*) hosted strikingly similar Symbiodiniaceae communities, with identical ITS2 types found across comparable environmental gradients (Naugle et al., 2024). RDA suggest that temperature was the primary driver, although other important factors such as light and turbidity (Cooper et al., 2011) were likely excluded due to multicollinearity. It remains also unclear whether *A. spathulata* associates with specific Symbiodiniaceae because these taxa are the most abundant at these locations, because they form the best performing symbioses (Bhattacharya et al., 2024), or both—since their relative abundance in the environment is unknown.

The spatial distribution of Symbiodiniaceae suggests some taxa may be environmental specialists while others may be environmental generalists. Similar to Epstein et al. (2019), we found *A. spathulata* associated with a C3k taxon at cooler offshore Central/Northern GBR reefs, and we also revealed a distinct C50c taxon predominant at warmer turbid inshore Central/Northern reefs. Conversely, C3k/C3bo appears to have a wide distribution as it was indistinguishable based on genome-sequence composition between NC and CB. Taxa from the C50b subclade, found across a 13° longitudinal gradient, might also be widespread in this region but best performing at high-latitudes. Importantly, these findings show that phylogenetic relatedness does not necessarily imply similar ecological niches, as the C50c and C50b populations were found in warmer and cooler environments respectively.

Broadcast spawners maintain long-distance asymmetrical gene flow across the Western Pacific

Demographic models detected substantial historical gene flow between Western Pacific populations separated by thousands of kilometers, that likely started to diverge between 0.275 to 0.651 MYA. While this potential connectivity had been suggested by biophysical models of coral dispersal (Wood et al., 2014), it remained to be empirically tested due to their potential biases (Saint-Amand et al., 2023). Although some uncertainty remained in the absolute values of gene flow, primary directions of migration rates were consistent across bootstrap replicates for all population pairs and these models had stronger support than divergence without gene flow.

On the GBR, gene flow was primarily southward, consistent with the predominant EAC direction and other studies on coral broadcast spawners (Matz et al., 2018; Meziere et al., 2025; Riginos et al., 2019). We also observed admixture between the Central/Northern and Southern GBR populations indicating recent southward migration between these regions (Figure 1). Conversely, gene flow was largely symmetrical between the GBR and Coral Sea atolls, reflecting the region's complex oceanography, which includes westward currents such as the North Caledonia Jet (NCJ) and the South Caledonia Jet (SCJ; Cravatte et al., 2015), as well as the eastward Sub Tropical Counter Current (STCC; Marchesiello et al., 2010). Demographic models inferred dominant eastward gene flow from the GBR to NC, and from CB to NC, which is unexpected given the prevailing westward NCJ and SCJ

621 in the region (Cravatte et al., 2015). These patterns of realized connectivity may have been influenced
622 by surface circulation associated with the STCC, while the strong NCJ and SCJ reach their maximum
623 intensity in deeper layers (Marchesiello et al., 2010). Observations of plastic debris and Lagrangian
624 dispersal modeling notably suggest that mesoscale currents can generate eastward drift in the region
625 despite the dominance of westward zonal jets (Maes & Blanke, 2015). Because gene flow inferred
626 from demographic models reflects an average across thousands of generations, these estimates could
627 also have been influenced by temporal changes in ocean circulation. Together, these results provide
628 novel insights into a complex realized connectivity across this region and highlight the value of such
629 analyses for informing management in contexts of variable ocean circulation. Beyond uncertainties in
630 the current directionality of gene flow, the models strongly support low but persistent migration
631 between these western Pacific populations. As such, they should be treated as distinct management
632 units (Hohenlohe et al., 2021) within a broader regional network that also recognizes the importance
633 of their connectivity for evolutionary adaptive potential.

634 *Large breeding population and high dispersal may support demographic resilience*

635 The effective population size of *A. spathulata* at the neighorhood size was relatively high (N_e=2,950)
636 despite drastic coral mortality over last decades (Eddy et al., 2021; Souter et al., 2021). This estimate
637 is particularly important for its conservation, as emphasized by the recent Kunming-Montreal Global
638 Biodiversity Framework (Waples, 2024). Although there is no exact rule of how large N_e should be,
639 our estimate suggests that local breeding populations are sufficiently large to prevent dramatic loss of
640 genetic diversity due to genetic drift (Waples, 2024). In contrast, brooding species with limited
641 dispersal and local recruitment tend to have lower N_e and higher local extinction risk (Hernández-
642 Agreda et al., 2024; Meziere et al., 2025; Prata et al., 2024).

643 High N_e likely reflects substantial census sizes of this common species densely distributed on reef flats
644 and slopes, combined with a large generation dispersal estimated at ~100km per generation. This
645 estimate contains some level of uncertainty because IbD theory assumes symmetrical dispersal across
646 a continuous habitat of constant population density, which does not match the typical patchiness of
647 coral reefs. Yet, this value is consistent with a pelagic larval duration estimated from lipid reserves at

~100 days which would allow larvae to be carried across large distances (Graham et al., 2013). Estimates from previous studies using similar methods vary from a few meters in brooding species (Gorospe & Karl, 2013; Hernández-Agreda et al., 2024; Prata et al., 2024) to 1–52 kilometers in broadcast spawning species (Japaud et al., 2019; Meziere et al., 2025). Our estimate also falls at the upper end of broadcast-spawners connectivity predicted by biophysical models (63% of settlement within 100km; Wood et al., 2014) and is comparable to coral trout dispersal on the GBR (Williamson et al., 2016). These findings suggest that *A. spathulata* exhibits one of the highest coral dispersal distances recorded to date. Importantly, we only estimated a global isotropic σ because IbD was not significant within populations but this estimate could vary among regions. Even if σ is similar across regions, the demographic consequences could differ because the GBR is a fragmented mosaic of numerous discrete reefs while NC and CB contain longer continuous barrier reefs (Andréfouët et al., 2009). Individual reefs are expected to be demographically isolated when separated by more than 2σ (Pinsky et al., 2012) and thus connectivity could differ between these reef systems of contrasting geomorphology.

Large N_e and high dispersal may explain the impressive recovery of *Acropora* communities on many GBR reefs after the 2016–2017 bleaching-related mortality events (Emslie et al., 2024), and will be critical for demographic recovery under increasingly frequent disturbances (Hock et al., 2017). For example, marine heat waves and freshwater floods caused 90–100% mortality of *A. spathulata* colonies at several inshore Northern GBR sites sampled in this study in 2024, while colonies at offshore reefs were relatively unaffected. Larval dispersal from these populations could thus in theory supply larvae to degraded reefs. However, a finer assessment of realized dispersal is needed to evaluate the inbound and outbound connectivity of individual reefs, as it depends on meso-scale currents and habitat availability. Finally, given the ongoing impacts to these populations from global warming, monitoring possible changes in N_e will be important to track changes in their vulnerability (Howells et al., 2022).

Habitat-specific symbioses and long-range dispersal affect the evolutionary adaptive potential of A. spathulata

675 *A. spathulata* formed distinct symbioses with Symbiodiniaceae across distinct thermal conditions
676 which raises the question of whether shifts to more heat-tolerant symbioses could promote the
677 adaptation of *A. spathulata* to rapid climate warming. *Acropora* corals symbioses with heat tolerant
678 symbionts—notably from the *Durusdinium* genus—have been observed to increase in prevalence
679 during marine heatwaves but this response appears to be species-specific and has not been yet reported
680 for *A. spathulata* (Quigley et al., 2022). The absence of *Durusdinium* in colonies sampled outside
681 major marine heatwaves in Epstein et al. (2019) and in our study suggests this association is
682 uncommon in *A. spathulata* under normal conditions. However, we observed variable symbioses
683 among colonies at mid-shelf reefs on the GBR, suggesting that both the C50c and C3k taxa are found
684 in these environments. Under future climate warming, symbioses with C50c typically found in warmer
685 inshore environments may become more prevalent on mid-shelf reefs, especially given that fast
686 growing *Acropora* corals can rapidly shift to better adapted symbionts within 1–2 years (Turnham et
687 al., 2025). Whether this ability varies across regions remains an open question, especially given that
688 the same C3k/C3bo taxon was found in colonies both from NC and CB reefs despite drastically
689 different environments. The absence of other associations may indicate lower potential for adaptation
690 through shifts in symbioses, or on the contrary indicate greater physiological plasticity and resilience
691 to changing conditions of this symbiont taxon. Further sampling around bleaching events is thus
692 needed to assess whether this species can shift symbioses quickly enough to reduce coral mortality
693 over future marine heatwaves.

694 Another factor that may underlie the evolutionary adaptation of *A. spathulata is the* long-distance gene
695 flow between western Pacific populations, as it could increase genetic variation or introduce heat-
696 tolerant alleles from warmer to cooler regions (Matz et al., 2020). On the GBR, dominant southward
697 gene flow may allow this process, as observed in other coral taxa (Matz et al., 2018; Meziere et al.,
698 2025; Riginos et al., 2019), particularly given that admixture suggest recent southward migration.
699 Among other populations, the effect of gene flow on adaptive genetic variation may be harder to
700 predict due to more-complex patterns. For example, the southern GBR showed substantial
701 northeastward gene flow toward CB populations typically found in warmer environments.

Nevertheless, occasional long-distance gene flow will benefit populations' adaptive potential by introducing novel genetic variation without swamping adaptive local variants (Fitzpatrick et al., 2020). We only inferred broad-scale patterns of gene flow among the four regions. Sampling a continuum of reefs in these regions and modeling gene flow at a finer resolution among reef groups (e.g., Matz et al., 2018; Meziere et al., 2025), along with construction of high-resolution biophysical models (e.g., Mason et al., 2025), would help building finer networks of reef connectivity (Mumby et al., 2021).

Within regions, high level of gene flow will constrain evolution by preventing strong local adaptation, for instance along cross-shore gradients. However, it will also facilitate the spread of standing genetic variation, as evidenced by limited differences in genetic diversity between reefs and regions. This gene flow will reduce the risk of inbreeding depression and enable the rapid spread of novel genetic variants across the population range (Slatkin, 1987). Future work investigating the distribution of adaptive genetic variation in this species will help clarify this ambivalent effect.

Conclusion

The genetic structure of the Western Pacific coral *A. spathulata* reflects opposing forces of geographic isolation and long-distance dispersal driven by major regional ocean currents. In parallel, variation in associated *Cladocopium* taxa along latitudinal and cross-shore environmental gradients suggests environmental filtering of symbioses. Our results enable the definition of management units across the Western Pacific, and emphasize the importance of considering coral reefs connectivity at the regional scale beyond national borders—as maintaining gene flow between distant populations could underlie their evolutionary adaptation (Fitzpatrick et al., 2020). The distinct spatial scales at which evolutionary processes affect coral hosts and their symbionts are also essential to consider for many proposed intervention approaches such as assisted gene flow, selective breeding or symbiont manipulations (van Oppen et al., 2017). Our findings indicate substantial effective population size and exceptional dispersal in *A. spathulata* that may support demographic rescue following disturbances, provided some locations remain unaffected. However, this study only offers a snapshot of the demographic status of *A. spathulata* populations. In light of the recent severe coral mortality events (Cantin et al., 2024), future reassessment of their vulnerability will be essential for effective conservation.

729

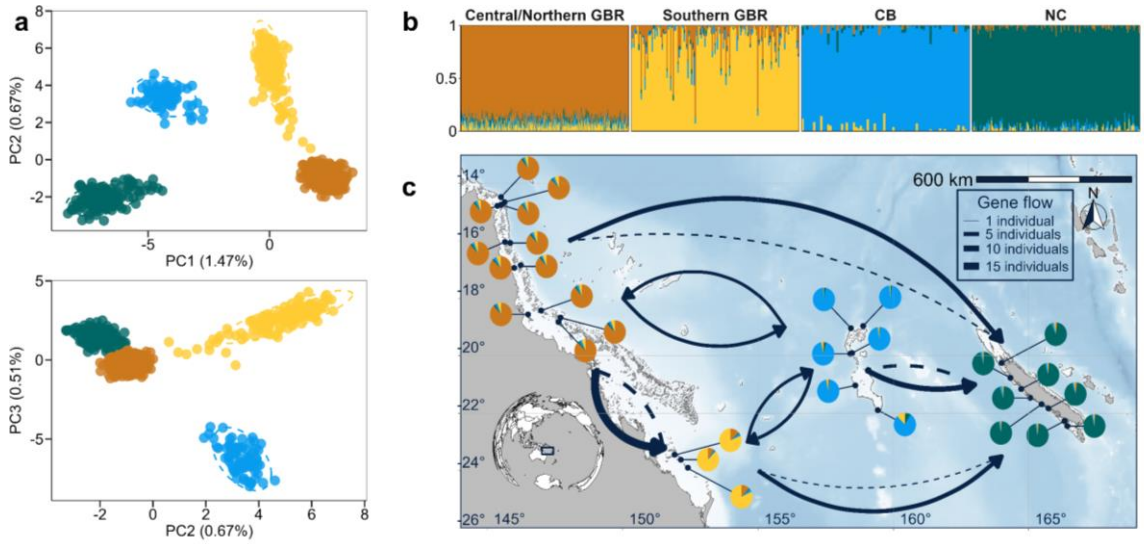

Figure 1. Population genomic structure and connectivity of *Acropora spathulata* across reefs from the Great Barrier Reef, Chesterfields-Bellona atolls (CB) and New Caledonia (NC). (a) Principal component analysis based on 27,175 SNPs showing four genetically and geographically distinct populations across the western Pacific. PC1, PC2 and PC3 are shown with the proportion of variance explained by each component indicated in percentages. (b) Ancestry proportions from each individual using ADMIXTURE analysis with the optimal number of ancestral populations found using cross-validation (K=4). (c) Map showing ancestry proportion at sampling sites, averaged across colonies (n=4–60). Arrows indicate average gene flow, in number of migrants per generation, between populations since their divergence inferred from demographic modeling in dadi. Solid and dashed lines indicate the primary and secondary directions of gene flow, respectively.

Table 1. Demographic modeling of *Acropora spathulata* populations divergence across the western Pacific. For each pair of populations (1: left, 2: right), optimized parameters are presented for the model exhibiting the best fit to the observed joint allelic frequency spectrum (divergence with asymmetrical gene flow) along with genetic differentiation statistics (fixation index F_{st} and absolute divergence D_{xy}). Nref, ν_1, ν_2 are the ancestral and current effective population sizes in thousands of individuals. m is the proportion of migrants per generation and M is the number of migrants per

generation. T is the estimated divergence time in thousands of years. For each model and parameter, median and 2.5–97.5% confidence intervals based on 100 optimized bootstrap replicates are presented.

Population pair	**Nref**	ν_1	ν_2	T	D_{XY}
Central/Northern GBR-Southern GBR	7.2 [4.1, 10.6]	63.9 [51.1, 76.3]	32.5 [25.9, 42.3]	276 [231, 320]	0.0102
Central/Northern GBR-NC	9.2 [5.1, 17.6]	82.9 [66.9, 118.9]	25.0 [14.5, 33.6]	323 [218, 379]	0.0107
Central/Northern GBR-CB	4.9 [3.7, 9.9]	61.9 [51.1, 75.8]	29.6 [21.6, 36.6]	354 [292, 373]	0.0102
Southern GBR-NC	6.5 [4.6, 10.9]	82.0 [73.6, 87.9]	32.8 [28.4, 39.5]	436 [378, 461]	0.0107
Southern GBR-CB	7.1 [4.4, 12.3]	65.8 [58.1, 74.5]	34.8 [28.6, 43.9]	395 [334, 431]	0.0100
NC-CB	7.2 [6.6, 9.9]	86.5 [76.4, 96.7]	48.8 [35.2, 56.1]	651 [630, 666]	0.0104
Population pair	**m_{12} (2→1)**	**m21 (1→2)**	**M1→2 ($N_e m_{12}$)**	**M21 ($N_e m_{21}$)**	F_{st}
Central/Northern GBR-South GBR	6.2e-5 [4.6e-5, 8.7e-5]	2.5e-4 [2.0e-4, 3.0e-4]	7.9 [6.6, 9.6]	16.4 [14.7, 18.0]	0.014
Central/Northern GBR-NC	2.1e-5 [9.4e-6, 3.5e-5]	2.0e-4 [1.5e-4, 3.0e-4]	3.6 [2.3, 4.7]	9.9 [8.6, 11.0]	0.025
Central/Northern GBR-CB	5.4e-5 [3.7e-5, 7.2e-5]	1.2e-4 [9.2e-5, 1.7e-4]	6.5 [5.2, 8.0]	7.1 [6.5, 7.8]	0.028
Southern GBR-NC	1.7e-5 [1.3e-5, 2.5e-5]	1.4e-4 [1.2e-4, 1.5e-4]	2.8 [2.2, 3.7]	8.8 [8.2, 9.5]	0.029
Southern GBR-CB	5.1e-5 [3.5e-5, 7.1e-5]	9.3e-5 [5.9e-5, 1.2e-4]	6.8 [5.1, 8.6]	6.3 [5.1, 7.3]	0.026
NC-CB	6.5e-5 [5.2e-5, 7.3e-5]	7.0e-5 [5.6e-5, 1.1e-4]	11.0 [9.8, 12.1]	6.9 [6.2, 7.8]	0.026

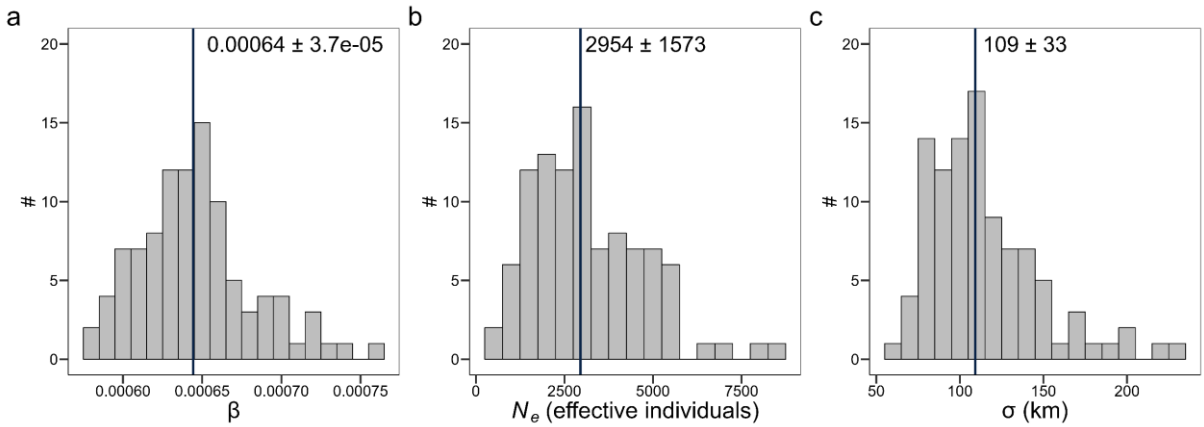

Figure 2. Generational dispersal and effective population size in *Acropora spathulata* from the western Pacific. Isolation by distance at multiple appropriate spatial scales was used to infer the distribution of (a) slope of genetic distance on geographic distance regressions, (b) effective population size at the neighborhood size and (c) mean axial generational dispersal distance. Vertical lines indicate the median of each distribution with median and standard deviation values indicated next to it.

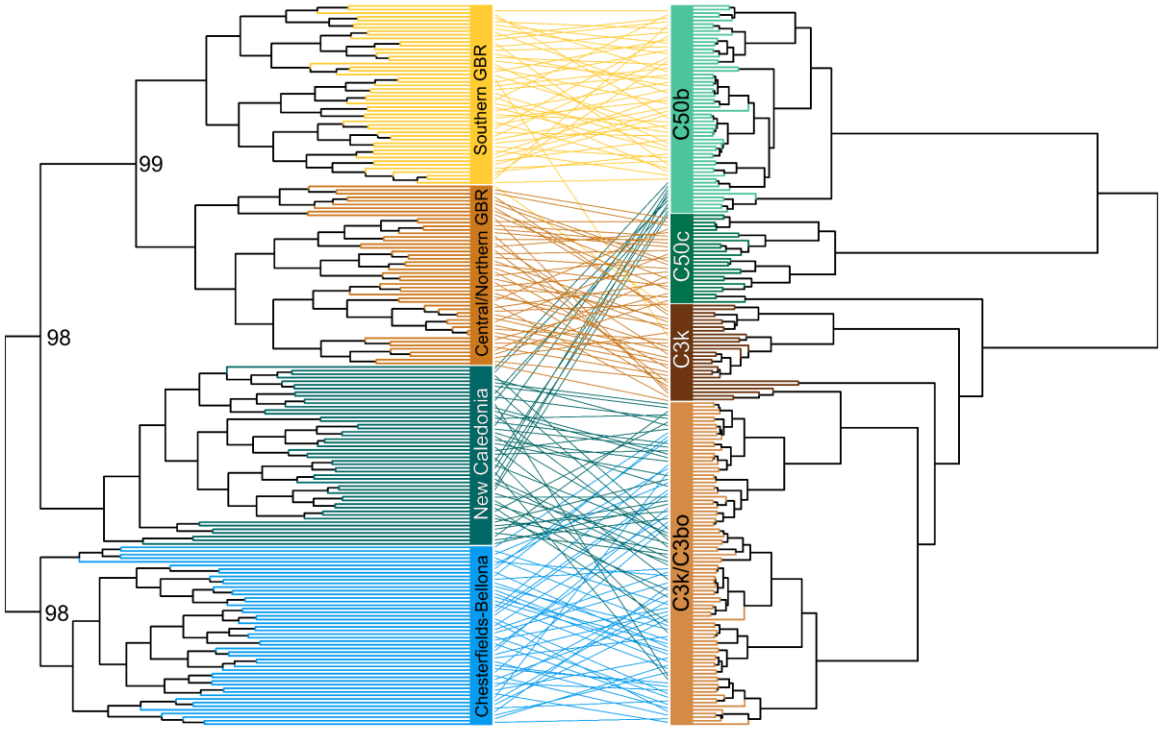

Figure 3. Co-clustering of *Acropora spathulata* coral hosts and associated Symbiodiniaceae taxa across the western Pacific. The host dendrogram (left) is a maximum likelihood tree derived from 27,175 SNPs using RAxML. The node values represent bootstrap support (>90) from 100 bootstrap replicates and branches are coloured based on ADMIXTURE ancestral populations. The symbiont dendrogram (right) is obtained through hierarchical clustering of the D_2^s distance matrix based on symbiont *k*-mer profiles and branches are colored according to majority ITS2 sequences for each sample.

Table 2. The influence of geography and environmental conditions on host neutral genetic structure of *Acropora spathulata* and the influence of geography, environmental conditions and host structure on associated Symbiodiniaceae communities. The relative influence of each category of predictors was decomposed using partial redundancy analysis (pRDA). Geography was modeled using distance-based Moran's Eigenvector maps. Environmental variables included factors indicative of temperature, irradiance, and turbidity.

Host model				
Partial RDA models	**Inertia**	**R^2 (Total Variance explained)**	***p*(>*F*)**	**Proportion of constrained variance explained**
Host PC ~ Env + Geography	21.38	0.701	0.001***	1
Host PC ~ Geography | Env	1.898	0.06	0.001***	0.089
Host PC ~ Env | Geography	0.987	0.03	0.001***	0.046
Confounded Env/Geography		0.611		0.865
Total unexplained	9.08	0.29		
Total inertia	30.46	1		
Symbiont model				
Partial RDA models	**Inertia**	**R^2 (Total Variance explained)**	***p*(>*F*)**	**Proportion of constrained variance explained**
Kmer ~ Env + Geography + Host_structure | (Nreads)	0.174	0.40	0.01**	1
Kmer ~ Env | (Nreads + Host_structure + Geography)	0.027	0.063	0.01**	0.15
Kmer ~ Geography | (Nreads +Env + Host structure)	0.005	0.012	0.01**	0.03
Kmer ~ Host_structure | (Nreads +Env + Geography)	0.004	0.01	0.01**	0.02
Confounded Env/Geography/Host structure		0.315		0.8
Total unexplained	0.167	0.6		
Total inertia	0.435	1		

774

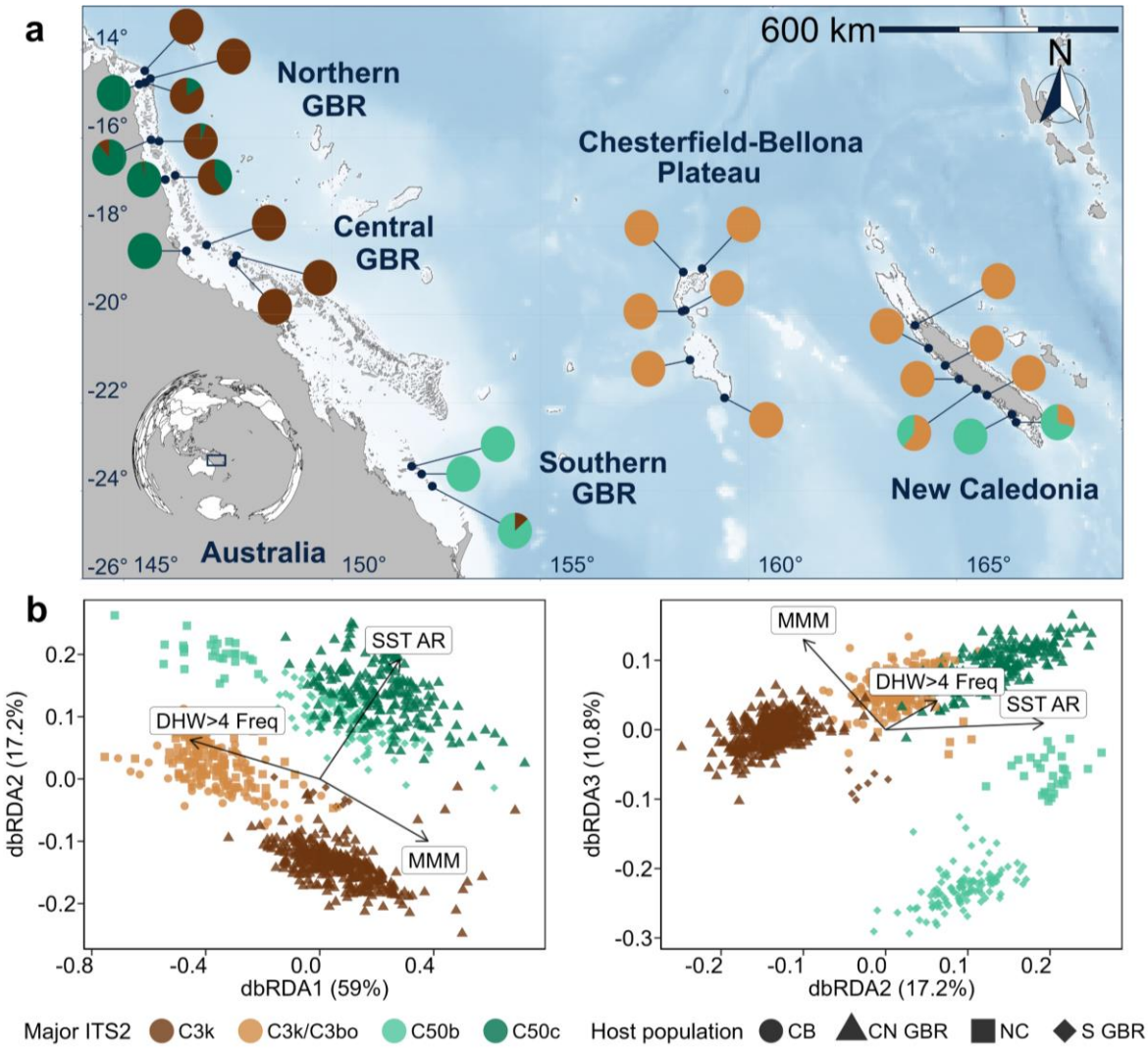

Figure 4. Variation in the symbiont (Symbiodiniaceae) communities of *Acropora spathulata* across geographic and environmental gradients in the western Pacific. (a) Map showing the proportion of colonies harboring each of the symbiont clusters identified using ordination of D_2^s distance matrix at each sampling site. Symbiont genetic clusters are coloured and labelled based on their major ITS2 type. (b) Distance-based redundancy Analysis (db-RDA) ordination of D_2^s *k*-mer profiles. Each individual is coloured by its major ITS2 sequence and the shape corresponds to each of the host populations (CN GBR = Central/Northern GBR, S GBR = Southern GBR, NC = New Caledonia, CB = Chesterfields-Bellona). Arrows represent significant environmental variables in the model. The first three axes explaining 87% of the constrained variance are shown.

Resource availability

Lead Contact

Requests for further information and resources should be directed to and will be fulfilled by the lead contact, Hugo Denis (**denis.hugo08@gmail.com**).

Data and code availability

Raw sequence data and unfiltered VCF file from this study will be made available on NCBI upon publication (BioProject XXX and BioProject XXX) and associated sample metadata can be accessed on GEOME (https://geome-db.org/record/ark:/21547/GPk2 and https://geome-db.org/record/ark:/21547/GLz2). Scripts used for WGS data processing and analyses are available on GitHub (https://github.com/hde08/Aspat_CoralSea_Popgen) and will be archived on Zenodo upon publication (XXX). Any additional information required to reanalyze the data reported in this paper is available from the lead contact upon request.

Acknowledgements

We thank the Traditional Owners of the Great Barrier Reef and New Caledonia reefs for their free prior and informed consent to undertake coral sampling in their Sea Country. We thank the government of New Caledonia for granting permission to conduct coral sampling within the Natural Park of the Coral Sea, as well as the South Province and North Province. We thank Samantha Goyen, Riverside Marine Cruise crew members and numerous AIMS staff and volunteers for their support while collecting on the GBR. We thank the French National Navy, Mahé Dumas, Bertrand Bourgeois, William Roman, Jordi Giraud and Martin Nguyen for their help while collecting in Chesterfield-Bellona atolls and New Caledonia Grande Terre. We thank Samantha Howitt for assisting in the DNA extractions at the University of Queensland and Clarisse Majorel for assisting in the DNA extractions in New Caledonia. We thank Molly Przeworski for providing an upgraded reference genome assembly. We thank Jérôme Lefèvre and Christophe Charbuillet for their support with HPC systems. This research was undertaken with the assistance of resources from the National Computational Infrastructure (NCI Australia), an NCRIS-enabled capability supported by the Australian Government,

through Project d85 awarded to C.X.C. Finally, we are thankful to Ryan Gutenkunst for his advice on demographic modeling analyses.

Authors contributions

V.B.L., E.J.H., L.K.B., C.R. and H.D. initiated the project and planned the sampling campaign. Fieldwork was done by H.D., L.K.B., V.M. and E.H. on the GBR and H.D., V.B.L., M.B. and G.L. in New Caledonia. DNA extractions were performed by I.B. and K.E.P. for GBR samples, and by H.D for New Caledonia samples. Whole genome sequence data was curated and analyzed by H.D. following a pipeline designed by I.P. Host population structure and phylogenetic analyses were performed by H.D. supported by I.P, K.E.P., C.R., E.J.H., G.L. and V.B.L. Demographic modeling analyses were performed by H.D. supported by K.E.P. IbD analyses were performed by K.E.P. Analyses of symbiont communities were performed by H.D. supported by H.I and C.X.C. H.D. wrote the first draft version of the manuscript which was critically revised by all co-authors. All authors read and approved the final manuscript.

Competing interests

The authors declare no competing interests.

Funding information

Work undertaken in Australia was supported by the Reef Restoration and Adaptation Program funded by the partnership between the Australian Government's Reef Trust and the Great Barrier Reef Foundation. Work in New Caledonia was supported by CNRS and IRD fundings and was part of the WINREEF (Reef Resilient Initiative/ Neo Caledonia Biodiversity Agency funding) and ReCoVer (Pacific Funds) projects. CB samplings were achieved thanks to the support of the French Navy with the vessel D'Entrecasteaux. H.D. was supported by a PhD scholarship from ED129 at Sorbonne University. H.I. and I.B were supported by the University of Queensland Research Training Program scholarship.

References

Alessi, C., Lemonnier, H., Camp, E. F., Wabete, N., Payri, C., & Rodolfo Metalpa, R. (2024). Algal symbiont diversity in *Acropora muricata* from the extreme reef of Bouraké associated with resistance to coral bleaching. *PloS One*, *19*(2), e0296902.

Alexander, D. H., & Lange, K. (2011). Enhancements to the ADMIXTURE algorithm for individual ancestry estimation. *BMC Bioinformatics*, *12*, 1-6.

Alvarado-Cerón, V., Muñiz-Castillo, A. I., León-Pech, M. G., Prada, C., & Arias-González, J. E. (2022). A decade of population genetics studies of scleractinian corals: A systematic review. *Marine Environmental Research*, 105781.

Andréfouët, S., Cabioch, G., Flamand, B., & Pelletier, B. (2009). A reappraisal of the diversity of geomorphological and genetic processes of New Caledonian coral reefs: a synthesis from optical remote sensing, coring and acoustic multibeam observations. *Coral Reefs*, *28*, 691-707.

Armstrong, E. J., Lê-Hoang, J., Carradec, Q., Aury, J.-M., Noel, B., Hume, B. C. C., Voolstra, C. R., Poulain, J., Belser, C., Paz-García, D. A., Cruaud, C., Labadie, K., Da Silva, C., Moulin, C., Boissin, E., Bourdin, G., Iwankow, G., Romac, S., Agostini, S., . . . Wincker, P. (2023). Host transcriptomic plasticity and photosymbiotic fidelity underpin *Pocillopora* acclimatization across thermal regimes in the Pacific Ocean. *Nature Communications*, *14*(1), 3056. https://doi.org/10.1038/s41467-023-38610-6

Armstrong, K. C., Lippert, M., Hanson, E., Nestor, V., Cornwell, B., Walker, N. S., Golbuu, Y., & Palumbi, S. R. (2024). Fine-Scale Geographic Variation of *Cladocopium* in *Acropora hyacinthus* Across the Palauan Archipelago. *Ecology and Evolution*, *14*(12), e70650.

Arrigoni, R., Berumen, M. L., Mariappan, K. G., Beck, P. S., Hulver, A. M., Montano, S., Pichon, M., Strona, G., Terraneo, T. I., & Benzoni, F. (2020). Towards a rigorous species delimitation framework for scleractinian corals based on RAD sequencing: the case study of *Leptastrea* from the Indo-Pacific. *Coral Reefs*, *39*, 1001-1025.

Bhattacharya, D., Stephens, T. G., Chille, E. E., Benites, L. F., & Chan, C. X. (2024). Facultative lifestyle drives diversity of coral algal symbionts. *Trends in Ecology & Evolution*, *39*(3), 239-247.

Bolger, A. M., Lohse, M., & Usadel, B. (2014). Trimmomatic: a flexible trimmer for Illumina sequence data. *Bioinformatics*, *30*(15), 2114-2120.

Bongaerts, P., Cooke, I. R., Ying, H., Wels, D., den Haan, S., Hernandez-Agreda, A., Brunner, C. A., Dove, S., Englebert, N., & Eyal, G. (2021). Morphological stasis masks ecologically divergent coral species on tropical reefs. *Current Biology*, *31*(11), 2286-2298. e2288.

Borcard, D., & Legendre, P. (2002). All-scale spatial analysis of ecological data by means of principal coordinates of neighbour matrices. *Ecological modelling*, *153*(1-2), 51-68.

Bourne, D. G., Morrow, K. M., & Webster, N. S. (2016). Insights into the coral microbiome: underpinning the health and resilience of reef ecosystems. *Annual Review of Microbiology*, *70*, 317-340.

Boyd, J. A., Woodcroft, B. J., & Tyson, G. W. (2018). GraftM: a tool for scalable, phylogenetically informed classification of genes within metagenomes. *Nucleic Acids Research*, *46*(10), e59-e59.

Butler, C. C., Turnham, K. E., Lewis, A. M., Nitschke, M. R., Warner, M. E., Kemp, D. W., Hoegh-Guldberg, O., Fitt, W. K., van Oppen, M. J., & LaJeunesse, T. C. (2023). Formal recognition of host-generalist species of dinoflagellate (Cladocopium, Symbiodiniaceae) mutualistic with Indo-Pacific reef corals. *Journal of phycology*.

Camp, E. F., Suggett, D. J., Pogoreutz, C., Nitschke, M. R., Houlbreque, F., Hume, B. C., Gardner, S. G., Zampighi, M., Rodolfo-Metalpa, R., & Voolstra, C. R. (2020). Corals exhibit distinct patterns of microbial reorganisation to thrive in an extreme inshore environment. *Coral Reefs*, *39*(3), 701-716.

Cantin, N., James, N., & Stella, J. (2024). Aerial surveys of the 2024 mass coral bleaching event on the Great Barrier Reef. *Australian Institute of Marine Science, Townsville*, 2024-2004.

Capblancq, T., & Forester, B. R. (2021). Redundancy analysis: A Swiss Army Knife for landscape genomics. *Methods in Ecology and Evolution*, *12*(12), 2298-2309.

Chen, Y., Shah, S., Dougan, K. E., van Oppen, M. J., Bhattacharya, D., & Chan, C. X. (2022). Improved *Cladocopium goreaui* genome assembly reveals features of a facultative coral symbiont and the complex evolutionary history of dinoflagellate genes. *Microorganisms*, *10*(8), 1662.

Clobert, J. (2012). *Dispersal ecology and evolution*. Oxford University Press.

Colton, M. A., McManus, L. C., Schindler, D. E., Mumby, P. J., Palumbi, S. R., Webster, M. M., Essington, T. E., Fox, H. E., Forrest, D. L., & Schill, S. R. (2022). Coral conservation in a warming world must harness evolutionary adaptation. *Nature Ecology & Evolution*, *6*(10), 1405-1407.

Cooke, I., Ying, H., Forêt, S., Bongaerts, P., Strugnell, J. M., Simakov, O., Zhang, J., Field, M. A., Rodriguez-Lanetty, M., & Bell, S. C. (2020). Genomic signatures in the coral holobiont reveal host adaptations driven by Holocene climate change and reef specific symbionts. *Science Advances*, *6*(48), eabc6318.

Cooper, T. F., Berkelmans, R., Ulstrup, K. E., Weeks, S., Radford, B., Jones, A. M., Doyle, J., Canto, M., O'Leary, R. A., & van Oppen, M. J. (2011). Environmental factors controlling the distribution of Symbiodinium harboured by the coral *Acropora millepora* on the Great Barrier Reef. *PloS One*, *6*(10), e25536.

Cravatte, S., Kestenare, E., Eldin, G., Ganachaud, A., Lefèvre, J., Marin, F., Menkes, C., & Aucan, J. (2015). Regional circulation around New Caledonia from two decades of observations. *Journal of Marine Systems*, *148*, 249-271.

Danecek, P., Auton, A., Abecasis, G., Albers, C. A., Banks, E., DePristo, M. A., Handsaker, R. E., Lunter, G., Marth, G. T., & Sherry, S. T. (2011). The variant call format and VCFtools. *Bioinformatics*, *27*(15), 2156-2158.

Danecek, P., Bonfield, J. K., Liddle, J., Marshall, J., Ohan, V., Pollard, M. O., Whitwham, A., Keane, T., McCarthy, S. A., & Davies, R. M. (2021). Twelve years of SAMtools and BCFtools. *GigaScience*, *10*(2), giab008.

Davies, S., Treml, E., Kenkel, C., & Matz, M. (2015). Exploring the role of Micronesian islands in the maintenance of coral genetic diversity in the Pacific Ocean. *Molecular Ecology*, *24*(1), 70-82.

Davies, S. W., Moreland, K. N., Wham, D. C., Kanke, M. R., & Matz, M. V. (2020). *Cladocopium* community divergence in two *Acropora* coral hosts across multiple spatial scales. *Molecular Ecology*, *29*(23), 4559-4572.

Denis, H., Bay, L. K., Mocellin, V. J., Naugle, M. S., Lecellier, G., Purcell, S. W., Berteaux-Lecellier, V., & Howells, E. J. (2024a). Thermal tolerance traits of individual corals are widely distributed across the Great Barrier Reef. *Proceedings B*, *291*(2030), 20240587.

Denis, H., Selmoni, O., Gossuin, H., Jauffrais, T., Butler, C. C., Lecellier, G., & Berteaux-Lecellier, V. (2024b). Climate adaptive loci revealed by seascape genomics correlate with phenotypic variation in heat tolerance of the coral *Acropora millepora*. *Scientific Reports*, *14*(1), 22179.

Dougan, K. E., Bellantuono, A. J., Kahlke, T., Abbriano, R. M., Chen, Y., Shah, S., Granados-Cifuentes, C., van Oppen, M. J., Bhattacharya, D., & Suggett, D. J. (2024). Whole-genome duplication in an algal symbiont bolsters coral heat tolerance. *Science Advances*, *10*(29), eadn2218.

Dray, S., Blanchet, G., Borcard, D., Guenard, G., Jombart, T., Larocque, G., Legendre, P., Madi, N., Wagner, H. H., & Dray, M. S. (2018). Package 'adespatial'. *R package*, *2018*, 3-8.

Eddy, T. D., Lam, V. W., Reygondeau, G., Cisneros-Montemayor, A. M., Greer, K., Palomares, M. L. D., Bruno, J. F., Ota, Y., & Cheung, W. W. (2021). Global decline in capacity of coral reefs to provide ecosystem services. *One Earth*, *4*(9), 1278-1285.

Edmunds, P. J., & Riegl, B. (2020). Urgent need for coral demography in a world where corals are disappearing. *Marine Ecology Progress Series*, *635*, 233-242.

Emslie, M. J., Ceccarelli, D. M., Logan, M., Blandford, M. I., Bray, P., Campili, A., Jonker, M. J., Parker, J. G., Prenzlau, T., & Sinclair-Taylor, T. H. (2024). Changing dynamics of Great Barrier Reef hard coral cover in the Anthropocene. *Coral Reefs*, *43*(3), 747-762.

Epstein, H. E., Smith, H. A., Cantin, N. E., Mocellin, V. J., Torda, G., & van Oppen, M. J. (2019). Temporal Variation in the Microbiome of *Acropora* Coral Species Does Not Reflect Seasonality. *Frontiers in Microbiology*, *10*, 1775.

Ewels, P., Magnusson, M., Lundin, S., & Käller, M. (2016). MultiQC: summarize analysis results for multiple tools and samples in a single report. *Bioinformatics*, *32*(19), 3047-3048.

Fisher, R. A. (1930). *The genetical theory of natural selection* [doi:10.5962/bhl.title.27468]. Clarendon Press. https://doi.org/10.5962/bhl.title.27468

Fitzpatrick, S. W., Bradburd, G. S., Kremer, C. T., Salerno, P. E., Angeloni, L. M., & Funk, W. C. (2020). Genomic and fitness consequences of genetic rescue in wild populations. *Current Biology*, *30*(3), 517-522. e515.

Fuentes-Pardo, A. P., & Ruzzante, D. E. (2017). Whole-genome sequencing approaches for conservation biology: Advantages, limitations and practical recommendations. *Molecular Ecology*, *26*(20), 5369-5406.

Gaines, S. D., White, C., Carr, M. H., & Palumbi, S. R. (2010). Designing marine reserve networks for both conservation and fisheries management. *Proceedings of the National Academy of Sciences*, *107*(43), 18286-18293. https://www.ncbi.nlm.nih.gov/pmc/articles/PMC2972919/pdf/pnas.200906473.pdf

Galili, T., Simpson, G., Jefferis, G., Gallotta, M., & Renaudie, J. (2015). Package 'dendextend'.

Gleason, D. F., & Hofmann, D. K. (2011). Coral larvae: from gametes to recruits. *Journal of Experimental Marine Biology and Ecology*, *408*(1-2), 42-57.

González-Pech, R. A., Stephens, T. G., Chen, Y., Mohamed, A. R., Cheng, Y., Shah, S., Dougan, K. E., Fortuin, M. D., Lagorce, R., & Burt, D. W. (2021). Comparison of 15 dinoflagellate genomes reveals extensive sequence and structural divergence in family Symbiodiniaceae and genus *Symbiodinium*. *BMC Biology*, *19*, 1-22.

Gorospe, K. D., & Karl, S. A. (2013). Genetic relatedness does not retain spatial pattern across multiple spatial scales: Dispersal and colonization in the coral, *P ocillopora damicornis*. *Molecular Ecology*, *22*(14), 3721-3736.

Graham, E., Baird, A., Connolly, S., Sewell, M., & Willis, B. (2013). Rapid declines in metabolism explain extended coral larval longevity. *Coral Reefs*, *32*, 539-549.

Grupstra, C. G., Gómez-Corrales, M., Fifer, J. E., Aichelman, H. E., Meyer-Kaiser, K. S., Prada, C., & Davies, S. W. (2024). Integrating cryptic diversity into coral evolution, symbiosis and conservation. *Nature Ecology & Evolution*, *8*(4), 622-636.

Gutenkunst, R. N., Hernandez, R. D., Williamson, S. H., & Bustamante, C. D. (2009). Inferring the joint demographic history of multiple populations from multidimensional SNP frequency data. *PLoS Genetics*, *5*(10), e1000695.

Hardy, O. J., & Vekemans, X. (1999). Isolation by distance in a continuous population: reconciliation between spatial autocorrelation analysis and population genetics models. *Heredity*, *83*(2), 145-154.

Hardy, O. J., & Vekemans, X. (2002). SPAGeDi: a versatile computer program to analyse spatial genetic structure at the individual or population levels. *Molecular Ecology Notes*, *2*(4), 618-620.

Hemstrom, W., Grummer, J. A., Luikart, G., & Christie, M. R. (2024). Next-generation data filtering in the genomics era. *Nature Reviews Genetics*, 1-18.

Hernández-Agreda, A., Huckeba, J., Prata, K. E., Vermeij, M. J., & Bongaerts, P. (2024). Hybridization and inbreeding affect the survival of a critically endangered coral. *Current Biology*, *34*(21), 5120-5129. e5124.

Hijmans, R. J., Williams, E., Vennes, C., & Hijmans, M. R. J. (2017). Package 'geosphere'. *Spherical trigonometry*, *1*(7), 1-45.

Hoadley, K. D., Pettay, D. T., Lewis, A., Wham, D., Grasso, C., Smith, R., Kemp, D. W., LaJeunesse, T., & Warner, M. E. (2021). Different functional traits among closely related algal symbionts dictate stress endurance for vital Indo-Pacific reef-building corals. *Global Change Biology*, *27*(20), 5295-5309.

Hock, K., Wolff, N. H., Ortiz, J. C., Condie, S. A., Anthony, K. R., Blackwell, P. G., & Mumby, P. J. (2017). Connectivity and systemic resilience of the Great Barrier Reef. *PLoS Biology*, *15*(11), e2003355.

Hohenlohe, P. A., Funk, W. C., & Rajora, O. P. (2021). Population genomics for wildlife conservation and management. *Molecular Ecology*, *30*(1), 62-82.

Holbrook, S. J., Adam, T. C., Edmunds, P. J., Schmitt, R. J., Carpenter, R. C., Brooks, A. J., Lenihan, H. S., & Briggs, C. J. (2018). Recruitment drives spatial variation in recovery rates of resilient coral reefs. *Scientific Reports*, *8*(1), 7338.

Howells, E., Beltran, V., Larsen, N., Bay, L., Willis, B., & van Oppen, M. (2012). Coral thermal tolerance shaped by local adaptation of photosymbionts. *Nature Climate Change*, *2*(2), 116-120.

Howells, E. J., Bay, L. K., & Bay, R. A. (2022). Identifying, Monitoring, and Managing Adaptive Genetic Variation in Reef-Building Corals under Rapid Climate Warming. In M. J. H. van Oppen & M. Aranda Lastra (Eds.), *Coral Reef Conservation and Restoration in the Omics Age* (pp. 55-70). Springer International Publishing. https://doi.org/10.1007/978-3-031-07055-6_4

Hume, B. C., Smith, E. G., Ziegler, M., Warrington, H. J., Burt, J. A., LaJeunesse, T. C., Wiedenmann, J., & Voolstra, C. R. (2019). SymPortal: A novel analytical framework and platform for coral algal symbiont next-generation sequencing ITS2 profiling. *Molecular Ecology Resources*, *19*(4), 1063-1080.

Hume, B. C., Ziegler, M., Poulain, J., Pochon, X., Romac, S., Boissin, E., De Vargas, C., Planes, S., Wincker, P., & Voolstra, C. R. (2018). An improved primer set and amplification protocol with increased specificity and sensitivity targeting the Symbiodinium ITS2 region. *PeerJ*, *6*, e4816.

Ishida, H., Riginos, C., & Chan, C. X. (2024). Contaminant or goldmine? In silico assessment of Symbiodiniaceae community using coral hologenomes. *Frontiers in Protistology*, *2*, 1376877.

Japaud, A., Bouchon, C., Magalon, H., & Fauvelot, C. (2019). Geographic distances and ocean currents influence Caribbean *Acropora palmata* population connectivity in the Lesser Antilles. *Conservation Genetics*, *20*(3), 447-466.

Jokiel, P. L. (1990). Transport of reef corals into the Great Barrier Reef. *Nature*, *347*(6294), 665-667.

Jombart, T. (2008). adegenet: a R package for the multivariate analysis of genetic markers. *Bioinformatics*, *24*(11), 1403-1405.

Korneliussen, T. S., Albrechtsen, A., & Nielsen, R. (2014). ANGSD: analysis of next generation sequencing data. *BMC Bioinformatics*, *15*(1), 1-13.

Korunes, K. L., & Samuk, K. (2021). pixy: Unbiased estimation of nucleotide diversity and divergence in the presence of missing data. *Molecular Ecology Resources*, *21*(4), 1359-1368.

LaJeunesse, T., Bhagooli, R., Hidaka, M., DeVantier, L., Done, T., Schmidt, G., Fitt, W., & Hoegh-Guldberg, O. (2004). Closely related Symbiodinium spp. differ in relative dominance in coral reef host communities across environmental, latitudinal and biogeographic gradients. *Marine Ecology Progress Series*, *284*, 147-161.

LaJeunesse, T. C., Parkinson, J. E., Gabrielson, P. W., Jeong, H. J., Reimer, J. D., Voolstra, C. R., & Santos, S. R. (2018). Systematic revision of Symbiodiniaceae highlights the antiquity and diversity of coral endosymbionts. *Current Biology*, *28*(16), 2570-2580. e2576.

LaJeunesse, T. C., Smith, R. T., Finney, J., & Oxenford, H. (2009). Outbreak and persistence of opportunistic symbiotic dinoflagellates during the 2005 Caribbean mass coral 'bleaching' event. *Proceedings of the Royal Society B: Biological Sciences*, *276*(1676), 4139-4148. https://doi.org/doi:10.1098/rspb.2009.1405

Lawson, D. J., Van Dorp, L., & Falush, D. (2018). A tutorial on how not to over-interpret STRUCTURE and ADMIXTURE bar plots. *Nature Communications*, *9*(1), 3258.

Legendre, P., & Anderson, M. J. (1999). Distance-based redundancy analysis: testing multispecies responses in multifactorial ecological experiments. *Ecological Monographs*, *69*(1), 1-24.

Levin, R. A., Beltran, V. H., Hill, R., Kjelleberg, S., McDougald, D., Steinberg, P. D., & van Oppen, M. J. (2016). Sex, scavengers, and chaperones: transcriptome secrets of divergent *Symbiodinium* thermal tolerances. *Molecular Biology and Evolution*, *33*(9), 2201-2215.

Lewis, A. M., Butler, C. C., Turnham, K. E., Wham, D. F., Hoadley, K. D., Smith, R. T., Kemp, D. W., Warner, M. E., & LaJeunesse, T. C. (2024). The diversity, distribution, and temporal stability of coral 'zooxanthellae'on a pacific reef: from the scale of individual colonies to across the host community. *Coral Reefs*, *43*(4), 841-856.

Li, H., & Durbin, R. (2010). Fast and accurate long-read alignment with Burrows–Wheeler transform. *Bioinformatics*, *26*(5), 589-595.

Li, T., Yu, L., Song, B., Song, Y., Li, L., Lin, X., & Lin, S. (2020). Genome improvement and core gene set refinement of *Fugacium kawagutii*. *Microorganisms*, *8*(1), 102.

Lukoschek, V., Riginos, C., & van Oppen, M. J. (2016). Congruent patterns of connectivity can inform management for broadcast spawning corals on the Great Barrier Reef. *Molecular Ecology*, *25*(13), 3065-3080.

Maes, C., & Blanke, B. (2015). Tracking the origins of plastic debris across the Coral Sea: A case study from the Ouvéa Island, New Caledonia. *Marine Pollution Bulletin*, *97*(1-2), 160-168.

Marchesiello, P., Lefèvre, J., Vega, A., Couvelard, X., & Menkes, C. (2010). Coastal upwelling, circulation and heat balance around New Caledonia's barrier reef. *Marine Pollution Bulletin*, *61*(7-12), 432-448.

Marzonie, M. R., Nielsen, J. J., Bay, L. K., Bourne, D. G., Nitschke, M. R., Selmoni, O., & Harrison, H. B. (2025). Seascape Genomics Reveal Contrasting Population Structure in Sympatric and Congeneric Corals Across Thermal Clines. *Diversity and Distributions*, *31*(8), e70065.

Mason, R., Langlais, C., Uribe-Palomino, J., Tonks, M., Coman, F., Choukroun, S., Porobic, J., & Doropoulos, C. (2025). Reef-scale variation in larval supply and settlement: validating dispersal predictions with observations of coral larvae. *Authorea Preprints*.

Matias, A. M. A., Popovic, I., Thia, J. A., Cooke, I. R., Torda, G., Lukoschek, V., Bay, L. K., Kim, S. W., & Riginos, C. (2022). Cryptic diversity and spatial genetic variation in the coral *Acropora tenuis* and its endosymbionts across the Great Barrier Reef. *Evolutionary Applications*, *16*(2), 293-310.

Matz, M. V., Treml, E. A., Aglyamova, G. V., & Bay, L. K. (2018). Potential and limits for rapid genetic adaptation to warming in a Great Barrier Reef coral. *PLoS Genetics*, *14*(4), e1007220.

Matz, M. V., Treml, E. A., & Haller, B. C. (2020). Estimating the potential for coral adaptation to global warming across the Indo-West Pacific. *Global Change Biology*, *26*(6), 3473-3481.

McRae, C. J., Keshavmurthy, S., Chen, H.-K., Ye, Z.-M., Meng, P.-J., Rosset, S. L., Huang, W.-B., Chen, C. A., Fan, T.-Y., & Côté, I. M. (2023). Baseline dynamics of Symbiodiniaceae genera and photochemical efficiency in corals from reefs with different thermal histories. *PeerJ*, *11*, e15421.

Meziere, Z., Popovic, I., Prata, K., Ryan, I., Pandolfi, J., & Riginos, C. (2024). Exploring coral speciation: Multiple sympatric *Stylophora pistillata* taxa along a divergence continuum on the Great Barrier Reef. *Evolutionary Applications*, *17*(1), e13644.

Meziere, Z., Prata, K., Lechene, M., Ferrari, R., Popovic, I., & Riginos, C. (2025). Connectivity differs by orders of magnitude among co-distributed corals, affecting spatial scales of eco-evolutionary processes. *Science Advances*, *11*(27), eadt2066.

Moore, R. B., Ferguson, K. M., Loh, W. K., Hoegh-Guldberg, O., & Carter, D. A. (2003). Highly organized structure in the non-coding region of the psbA minicircle from clade C Symbiodinium. *International journal of systematic and evolutionary microbiology*, *53*(6), 1725-1734.

Mumby, P. J., Mason, R. A., & Hock, K. (2021). Reconnecting reef recovery in a world of coral bleaching. *Limnology and Oceanography: Methods*, *19*(10), 702-713.

Nand, A., Zhan, Y., Salazar, O. R., Aranda, M., Voolstra, C. R., & Dekker, J. (2021). Genetic and spatial organization of the unusual chromosomes of the dinoflagellate *Symbiodinium microadriaticum*. *Nature Genetics*, 1-12.

Naugle, M. S., Denis, H., Mocellin, V. J., Laffy, P. W., Popovic, I., Bay, L. K., & Howells, E. J. (2024). Heat tolerance varies considerably within a reef-building coral species on the Great Barrier Reef. *Communications Earth & Environment*, *5*(1), 525.

Neel, M. C., McKelvey, K., Ryman, N., Lloyd, M. W., Short Bull, R., Allendorf, F. W., Schwartz, M. K., & Waples, R. S. (2013). Estimation of effective population size in continuously distributed populations: there goes the neighborhood. *Heredity*, *111*(3), 189-199.

Nitschke, M. R., Rosset, S. L., Oakley, C. A., Gardner, S. G., Camp, E. F., Suggett, D. J., & Davy, S. K. (2022). The diversity and ecology of Symbiodiniaceae: A traits-based review. *Advances in Marine Biology*, *92*, 55-127.

Oksanen, J., Blanchet, F. G., Kindt, R., Legendre, P., Minchin, P. R., O'hara, R., Simpson, G. L., Solymos, P., Stevens, M. H. H., & Wagner, H. (2013). Package 'vegan'. *Community Ecology Package, version*, *2*(9), 1-295.

Oury, N., Gélin, P., & Magalon, H. (2020). Cryptic species and genetic connectivity among populations of the coral *Pocillopora damicornis* (Scleractinia) in the tropical southwestern Pacific. *Marine Biology*, *167*(10), 1-15.

Pinsky, M. L., Palumbi, S. R., Andréfouët, S., & Purkis, S. J. (2012). Open and closed seascapes: Where does habitat patchiness create populations with high fractions of self-recruitment? *Ecological applications*, *22*(4), 1257-1267.

Prata, K. E., Bongaerts, P., Dwyer, J. M., Ishida, H., Howitt, S. M., Hereward, J. P., Crandall, E. D., & Riginos, C. (2024). Some reef-building corals only disperse metres per generation. *Proceedings B*, *291*(2027), 20231988.

Purcell, S., Neale, B., Todd-Brown, K., Thomas, L., Ferreira, M. A., Bender, D., Maller, J., Sklar, P., De Bakker, P. I., & Daly, M. J. (2007). PLINK: a tool set for whole-genome association and population-based linkage analyses. *The American Journal of Human Genetics*, *81*(3), 559-575.

Quigley, K. M., Ramsby, B., Laffy, P., Harris, J., Mocellin, V. J., & Bay, L. K. (2022). Symbioses are restructured by repeated mass coral bleaching. *Science Advances*, *8*(49), eabq8349.

Quigley, K. M., Willis, B. L., & Kenkel, C. D. (2019). Transgenerational inheritance of shuffled symbiont communities in the coral *Montipora digitata*. *Scientific Reports*, *9*(1), 1-11.

Reich, H. G., Kitchen, S. A., Stankiewicz, K. H., Devlin-Durante, M., Fogarty, N. D., & Baums, I. B. (2021). Genomic variation of an endosymbiotic dinoflagellate (*Symbiodinium* 'fitti') among closely related coral hosts. *Molecular Ecology*, *30*(14), 3500-3514.

Reinert, G., Chew, D., Sun, F., & Waterman, M. S. (2009). Alignment-free sequence comparison (I): statistics and power. *Journal of Computational Biology*, *16*(12), 1615-1634.

Riginos, C., Hock, K., Matias, A. M., Mumby, P. J., van Oppen, M. J., & Lukoschek, V. (2019). Asymmetric dispersal is a critical element of concordance between biophysical dispersal models and spatial genetic structure in Great Barrier Reef corals. *Diversity and Distributions*, *25*(11), 1684-1696.

Riginos, C., Popovic, I., Meziere, Z., Garcia, V., Byrne, I., Howitt, S. M., Ishida, H., Bairos-Novak, K., Humanes, A., & Scharfenstein, H. (2024). Cryptic species and hybridisation in corals: challenges and opportunities for conservation and restoration. *Peer Community Journal*, *4*, Article e106.

Rousset. (1999). Genetic differentiation between individuals. *Journal of Evolutionary Biology*, *13*(1), 58-62.

Rousset, F. (1997). Genetic differentiation and estimation of gene flow from F-statistics under isolation by distance. *Genetics*, *145*(4), 1219-1228.

Saint-Amand, A., Lambrechts, J., & Hanert, E. (2023). Biophysical models resolution affects coral connectivity estimates. *Scientific Reports*, *13*(1), 9414.

Scott, C. B., Schott, R., & Matz, M. V. (2024). Cryptic genetic structure of the coral host is the primary driver of holobiont assembly in massive *Porites*. *BioRxiv*, 2024.2001. 2009.574877.

Selmoni, O., Lecellier, G., Magalon, H., Vigliola, L., Oury, N., Benzoni, F., Peignon, C., Joost, S., & Berteaux-Lecellier, V. (2021). Seascape genomics reveals candidate molecular targets of heat stress adaptation in three coral species. *Molecular Ecology*, *30*(8), 1892-1906.

Shah, S., Dougan, K. E., Chen, Y., Lo, R., Laird, G., Fortuin, M. D., Rai, S. K., Murigneux, V., Bellantuono, A. J., & Rodriguez-Lanetty, M. (2024). Massive genome reduction predates the divergence of Symbiodiniaceae dinoflagellates. *The ISME Journal*, *18*(1), wrae059.

Shlesinger, T., & van Woesik, R. (2023). Oceanic differences in coral-bleaching responses to marine heatwaves. *Science of The Total Environment*, 162113.

Shoguchi, E., Shinzato, C., Kawashima, T., Gyoja, F., Mungpakdee, S., Koyanagi, R., Takeuchi, T., Hisata, K., Tanaka, M., & Fujiwara, M. (2013). Draft assembly of the *Symbiodinium minutum* nuclear genome reveals dinoflagellate gene structure. *Current Biology*, *23*(15), 1399-1408.

Slatkin, M. (1987). Gene flow and the geographic structure of natural populations. *Science*, *236*(4803), 787-792.

Sopniewski, J., & Catullo, R. A. (2024). Estimates of heterozygosity from single nucleotide polymorphism markers are context-dependent and often wrong. *Molecular Ecology Resources*, *24*(4), e13947.

Souter, D., Planes, S., Wicquart, J., Logan, M., Obura, D., & Staub, F. (2021). Status of coral reefs of the world: 2020. In: Global Coral Reef Monitoring Network (GCRMN) and International Coral Reef Initiative (ICRI).

Stamatakis, A. (2014). RAxML version 8: a tool for phylogenetic analysis and post-analysis of large phylogenies. *Bioinformatics*, *30*(9), 1312-1313.

Sully, S., Hodgson, G., & van Woesik, R. (2022). Present and future bright and dark spots for coral reefs through climate change. *Global Change Biology*, *28*(15), 4509-4522.

Tsuchiya, K., Zayasu, Y., Nakajima, Y., Arakaki, N., Suzuki, G., Satoh, N., & Shinzato, C. (2022). Genomic analysis of a reef-building coral, *Acropora digitifera*, reveals complex population structure and a migration network in the Nansei Islands, Japan. *Molecular Ecology*, *31*(20), 5270-5284.

Turnham, K. E., Lewis, A. M., Kemp, D. W., Warner, M. E., Wham, D. F., Smith, R. T., Hoadley, K., Colin, P. L., Golbuu, Y., & LaJeunesse, T. C. (2025). Limited persistence of the heat-tolerant zooxanthella, *Durusdinium trenchii*, in corals transplanted to a barrier reef where it is rare among natal colonies. *Coral Reefs*, 1-16.

Van der Auwera, G. A., & O'Connor, B. D. (2020). *Genomics in the cloud: using Docker, GATK, and WDL in Terra*. O'Reilly Media.

van Oppen, M. J., Bongaerts, P., Frade, P., Peplow, L. M., Boyd, S. E., Nim, H. T., & Bay, L. K. (2018). Adaptation to reef habitats through selection on the coral animal and its associated microbiome. *Molecular Ecology*, *27*(14), 2956-2971.

van Oppen, M. J., & Gates, R. D. (2006). Conservation genetics and the resilience of reef-building corals. *Molecular Ecology*, *15*(13), 3863-3883.

van Oppen, M. J., Gates, R. D., Blackall, L. L., Cantin, N., Chakravarti, L. J., Chan, W. Y., Cormick, C., Crean, A., Damjanovic, K., & Epstein, H. (2017). Shifting paradigms in restoration of the world's coral reefs. *Global Change Biology*, *23*(9), 3437-3448.

van Oppen, M. J., Palstra, F. P., Piquet, A. M.-T., & Miller, D. J. (2001). Patterns of coral–dinoflagellate associations in *Acropora*: significance of local availability and physiology of Symbiodinium strains and host–symbiont selectivity. *Proceedings of the Royal Society of London. Series B: Biological Sciences*, *268*(1478), 1759-1767.

Waples, R. (2024). The idiot's Guide to Effective Population Size. *Authorea Inc*, 1-51.

Waples, R. S., & Do, C. (2008). LDNE: a program for estimating effective population size from data on linkage disequilibrium. *Molecular Ecology Resources*, *8*(4), 753-756.

Warner, P. A., van Oppen, M. J., & Willis, B. L. (2015). Unexpected cryptic species diversity in the widespread coral *Seriatopora hystrix* masks spatial-genetic patterns of connectivity. *Molecular Ecology*, *24*(12), 2993-3008.

Weir, B. S., & Cockerham, C. C. (1984). Estimating F-statistics for the analysis of population structure. *Evolution*, 1358-1370.

Whitlock, M. C., & McCauley, D. E. (1999). Indirect measures of gene flow and migration: FST≠ 1/(4Nm+ 1). *Heredity*, *82*(2), 117-125.

Wickham, H. (2011). ggplot2. *Wiley Interdisciplinary Reviews: Computational Statistics*, *3*(2), 180-185.

Williamson, D. H., Harrison, H. B., Almany, G. R., Berumen, M. L., Bode, M., Bonin, M. C., Choukroun, S., Doherty, P. J., Frisch, A. J., & Saenz-Agudelo, P. (2016). Large-scale, multidirectional larval connectivity among coral reef fish populations in the Great Barrier Reef Marine Park. *Molecular Ecology*, *25*(24), 6039-6054.

Wood, S., Paris, C., Ridgwell, A., & Hendy, E. (2014). Modelling dispersal and connectivity of broadcast spawning corals at the global scale. *Global Ecology and Biogeography*, *23*(1), 1-11.

Wright, S. (1946). Isolation by distance under diverse systems of mating. *Genetics*, *31*(1), 39.

Zhang, J., Richards, Z. T., Adam, A. A., Chan, C. X., Shinzato, C., Gilmour, J., Thomas, L., Strugnell, J. M., Miller, D. J., & Cooke, I. (2022). Evolutionary responses of a reef-building coral to climate change at the end of the last glacial maximum. *Molecular Biology and Evolution*, *39*(10), msac201.